The rat ponto-medullary network responsible for paradoxical sleep onset and maintenance: a combined microinjection and functional neuroanatomical study.

Romuald Boissard, Damien Gervasoni, Markus H Schmidt, Bruno Barbagli, Patrice Fort, Pierre-Hervé Luppi

The rat ponto-medullary network responsible for paradoxical sleep onset and maintenance: a combined microinjection and functional neuroanatomical study

Romuald Boissard[1], Damien Gervasoni[1], Markus Schmidt[2], Bruno Barbagli[1], Patrice Fort[1] and Pierre-Hervé Luppi[1]‡

Address :   [1]CNRS FRE 2469, Institut Fédératif des Neurosciences de Lyon (IFR 19), Université Claude Bernard Lyon I, 8 Av Rockefeller, 69373 LYON Cedex 08, FRANCE
               [2]Ohio Sleep Medicine and Neuroscience Institute, 4975 Bradenton Ave., Dublin, Ohio 43017 and Adjunct Assistant Professor, The Ohio State University, Department of Neuroscience

Running Title : REM sleep brainstem structures in rats

Number of text pages : 46
Number of Figures : 12 Number of tables : 2
Numbers of words in the Abstract : 243
Introduction : 503
Manuscript : 70972

‡ Corresponding author

CNRS FRE 2469, Faculté de Médecine,
8 avenue Rockefeller, 69373 LYON cedex 08, FRANCE

Tel number   (+33) 4 78 77 71 71
Fax number   (+33) 4 78 77 71 72
E-mail   luppi@sommeil.univ-lyon1.fr

Key Words: REM sleep, glycine, GABA, subcoeruleus, C-Fos

Abstract

The neuronal network responsible for paradoxical sleep (PS) onset and maintenance has not been identified in the rat, unlike in the cat. To fill this gap, we developed a new technique involving the recording of sleep-wake states in unanaesthetized head-restrained rats while locally administering pharmacological agents by microiontophoresis from glass multi-barrel micropipettes into the dorsal pontine tegmentum combined with single unit recordings and functional neuroanatomy. Pharmacological agents used for iontophoretic administration included carbachol, kainic acid, bicuculline and gabazine. The injection sites and their efferents were then identified by injections of anterograde (Phaseolus leucoagglutinin) or retrograde (cholera toxin B subunit) tracers through an adjacent barrel of the micropipette assembly and by C-Fos immunostaining. Bicuculline, gabazine and kainic acid ejections specifically into the pontine sublaterodorsal nucleus (SLD) induced within a few minutes a PS-like state characterized by a continuous muscle atonia, low voltage EEG and a lack of reaction to stimuli. In contrast, carbachol ejections into the SLD induced wakefulness. In our PHA-L, glycine and C-Fos multiple double-labelling experiments, anterogradely-labelled fibers originating from the SLD were seen apposed on glycine and C-Fos positive neurones (labelled after 90 min of pharmacologically induced PS-like state) from the ventral gigantocellular and parvocellular reticular nuclei. Altogether, our data indicate that the SLD nuclei contain a population of neurones playing a crucial role in PS onset and maintenance. Furthermore, they suggest that GABAergic desinhibition and glutamate excitation of these neurones might play a crucial role in the onset of PS.

Introduction

In the middle of the last century, a series of historical observations lead to the discovery of a vigilance state in humans and other mammals paradoxically characterized by cortical activation and rapid eye movements, but associated with a complete disappearance of the muscle tone (Aserinsky and Kleitman, 1953; Dement, 1958; Jouvet and Michel, 1959). This phase of sleep, coined paradoxical sleep (PS) or rapid eye movement (REM) sleep was then demonstrated to correlate with dream activity (Aserinsky and Kleitman, 1953; Dement and Kleitmann, 1957).

Through a series of lesion, electrophysiological, local pharmacological and neuroanatomical studies, it has been shown in cats that a small area of the dorsal rostral pontine reticular nucleus (PRNr), named peri-locus coeruleus α (peri-LCα) by Sakai et al. (1979, 1981), contains the neurones responsible for PS. They are composed of presumed cholinergic and non-cholinergic neurones, with an activity specific to PS (PS-on neurones) (Sakai et al., 1981; Sakai et al., 2001). Some of these neurones project to the intralaminar nuclei of the thalamus (ILM), the posterior hypothalamus and the basal forebrain and may be responsible for the cortical activation during PS while others project caudally to the ventromedial medullary reticular formation (Sakai et al., 1979; Sakai et al., 1981; Review in Jones, 1991) and may generate the muscle atonia observed during this sleep state (Sakai et al., 2001).

With respect to the muscular atonia, the inhibitory amino acid glycine (gly) appears to play a major role in the tonic hyperpolarization of motoneurones during PS (Chase et al., 1989). Based on a number of neuroanatomical results (Luppi et al., 1988, Fort et al., 1990, 1993), we have proposed that non-cholinergic peri-LCα neurones induce the muscle atonia during PS via an excitatory projection to glycinergic premotoneurones localized in the ventromedial medullary reticular formation.

It has been suggested that the onset of activity of the non-cholinergic PS-on peri-LCα cells is due to an excitatory projection from cholinergic PS-on cells located in the peri-LCα, laterodorsal

tegmental (LDT) and pedunculopontine nuclei (PPN), as well as the removal of an inhibition from monoaminergic PS-off cells (Hobson et al., 1975; Siegel and McGinty, 1977; Sakai et al., 1981). This hypothesis is supported by the observation that carbachol administration into the peri-LCα induces PS in the cat (Vanni-Mercier et al., 1989) and that carbachol activates non-cholinergic PS-on neurones in this region (Sakai and Koyama, 1996). In rats however, pressure injections of carbachol in the dorsal part of the PRNr induce only a small PS hypersomnia (Gnadt and Pegram, 1986; Velazquez-Moctezuma et al., 1989; Bourgin et al., 1995; Deurveilher et al., 1997; Kubin, 2001). Moreover, PS-on neurones have not been recorded in this region and their medullary projections have not been demonstrated. Since the rat is now the animal of choice for experimental neurophysiology, we decided to identify the pontine neurones, as well as their projections, responsible for PS in this species by using a new model combining single unit recording, precise and limited local pharmacology by micro-iontophoresis, anterograde and retrograde tracing combined with C-Fos and neurotransmitter identification of labelled-cells.

Material and Methods

Fixation of the head-restraining system.

This procedure has in part been described previously (Darracq et al., 1996; Gervasoni et al., 1998, 2000, Soulière et al., 2000). Male Sprague-Dawley rats (280-320g, n=25, IFFA Credo, France) were anaesthetized with pentobarbital (45 mg/kg, i.p.) and mounted conventionally in a stereotaxic frame (David Kopf), i.e. with ear- and nose-bars. The bone was exposed and cleaned. The skull was placed at a 15° angle (nose tilted down) to avoid the transverse sinus overlying the pontine reticular formation during the subsequent electrode penetrations. Three stainless steel screws were fixed in the parietal and frontal parts of the skull and three wire electrodes inserted into the neck muscles to monitor the electroencephalogram (EEG) and the electromyogram (EMG), respectively. In some animals (n=11), two electrodes were implanted on both sides in the orbits for eye movement recordings (EOG). Penile erections (n=3) were recorded according to a technique previously described (Schmidt et al., 1994, 2000), involving chronic pressure monitoring within the bulb of the corpus spongiosum of the penis (CSP).

The bone was then covered with a thin layer of acrylic cement (Superbond, Sun Med. Co, Japan), except the region overlying the sublaterodorsal nucleus (SLD) and the lambdoid suture. At this time, the head-restraining system was put in place. It consists of a "U" shaped piece of aluminum with four bolts in each angle cemented to the skull of the rat, that can be easily fixed to a carriage, itself fastened to a commercial stereotaxic apparatus with dummy ear-bars. This device allows a painless stereotaxic restraint with high mechanical stability. The "U" piece fixed to the carriage with four bolts was centered above the SLD entry region and embedded in a mount of dental cement with the EEG screws and wires, and their 6-pin connector. After the dental cement dried out, the four bolts were then unscrewed from the U, now firmly jointed to the rat's skull. The animal was removed from the stereotaxic apparatus and allowed to recover from surgery and

anaesthesia for 48 hours, before beginning the habituation to the head-restrained apparatus. While in the head-restrained apparatus, rats are easily able to move their extremities. The head restraining system (5 g weight) was well tolerated by the rats and they were able to feed and drink normally in their home cages.

Training and habituation.

During 8-10 successive days, repetitive trials of increasing duration were done to well habituate the rats to the restraining and recording systems. A hammock comfortably supported the rat with the head painlessly secured to the restraining frame. At the end of the training period, the rats could stay calm for periods of 5 to 7 hours during which an alternance of quiet wake (W), slow wave sleep (SWS) and PS was routinely observed. Under pentobarbital anaesthesia, a 4 mm hole was made in the skull above the SLD and the dura was removed under microscopic control the day before the first recording session. The brain surface was cleaned at the beginning of each daily recording session under local lidocaine anaesthesia. All animals were housed and cared for according to the National Institute of Health "Guide for the Care and Use of Laboratory Animals" (NIH Publication 80-23). The protocol of this study has been approved by our local ethical committee and the French Ministry of Agriculture (Authorization n° 03-505), and efforts were made to reduce the number of animals used.

Local pharmacology.

For the majority of the local pharmacology experiments, a four barrels micropipette assembly was used.

For the bicuculline or gabazine experiments, one barrel was filled with bicuculline (10 mM, pH 4, Sigma) or gabazine (SR-95531, 5 mM, pH 3.8, Sigma), a second one with carbachol (100

mM, pH 4, Sigma), a third one with 2.5% phaseolus leucoaglutinin (PHA-L, Vector Lab, USA) or 0.5% cholera-toxin B subunit (CTb, List Biological Laboratories, USA) and the last one with NaCl 0.9%.

To determine whether the PS-like state obtained by bicuculline iontophoresis was due to an underlying constant excitation of SLD neurones by glutamate, the barrels were filled with bicuculline, kynurenic acid (200 mM, pH 8, Sigma) and NaCl 0.9%.

In the kainic acid experiments, one barrel was filled with carbachol, the second with kainic acid (500 µM, pH 8-9, Sigma), a third with PHA-L or CTb and the last with NaCl 0.9%.

The pharmacological agents were dissolved in distilled water, CTb in phosphate buffer 100 mM pH 6.0 and PHA-L in 10 mM phosphate-buffered saline pH 8.0. In all cases, small retention currents (2-5 nA) were used to avoid leakage of the active substances by diffusion. Current balancing techniques and current tests (Stone, 1985) were routinely done via the saline-containing barrel.

Before starting the local pharmacology, a single recording glass micropipette (3-5 µm tip diameter) was lowered at the stereotaxic coordinates of the right SLD (Swanson, 1992). The micropipettes were placed on the brain surface 3.5 mm posterior to the lambda, 1.2 mm lateral to the midline. Neurones specifically active during PS were found 6500-7000 µm below brain surface, and 500µm ventral to rostral locus coeruleus nucleus (LC) or mesencephalic trigeminal nucleus (MEV). LC noradrenergic neurones were characterized by their specific activity during waking (Gervasoni et al., 1998). The activity of the MEV neurones was correlated with jaw movements. Neurones with an activity specific to PS were recorded as long as possible across different sleep-wake episodes. Neurones with a different type of activity were not further considered.

After the initial period of localization of the target area, requiring at least one day of recording, a multibarrel micropipette was lowered into the right SLD every day. In the first pilot studies, the current intensities and durations of kainic acid, carbachol, bicuculline and gabazine iontophoretic ejections giving rise to reproducible and reversible effects were determined. It was

found that applications for 5 min of kainic acid and for 15 or 90 min of gabazine and bicuculline with a current intensity of 100 nA induced a sustained PS-like state while 50 nA applications did not reliably induced such effect. Applications of kainic acid, bicuculline or gabazine with 200 nA current induced a PS-like state rapidly disrupted by agitated waking. Kainic acid ejections during 5 min induced a PS-like state followed by a long-lasting agitated waking. Carbachol applications with 50 nA current induced no effect whereas waking was induced using 100-400 nA current. In view of these results, kainic acid, bicuculline and gabazine were subsequently ejected with 100 nA and carbachol with 100-200 nA.

In the subsequent experiments, bicuculline, gabazine, carbachol or kainic acid were ejected in the SLD and surrounding regions after one hour of rest. When the ejection induced a PS like-state, we waited for one hour after the end of the effect. Then, either a second injection was made 500 to 1000 µm away from the first site ventro-dorsally, rostro-caudally or medio-laterally or carbachol was ejected in the positive site. In some cases, carbachol ejections were done first before bicuculline or gabazine applications to avoid desensitizing effects. When the first ejection gave rise to a negative result, a second ejection was made one hour later 500 µm away in one direction from the first site. Successive ejections were done until the positive site was localized.

In the set of experiments with co-applications of bicuculline and kynurenic acid, bicuculline was first applied alone in the SLD for at least 5 min. Then, kynurenic acid was ejected during 3-10 min leaving an interval of at least 11 min between two ejections.

The first time a positive effect was obtained, PHA-L was ejected before moving the electrode with a current of 5 µA 7sec on/off for 15 min and continuously for another 15 min. During experiments on subsequent days, one of the barrels of the micropipette was filled with CTb. The CTb was ejected with a current of 1 µA 7sec on/off during 15 min after a positive effect was obtained. During the next seven days, no tracer was put into the multibarrels used for local pharmacology. Around the eighth day after the ejection of CTb, one barrel of the micropipette assembly was filled with 2% (w/v) pontamine sky blue (PSB) in 0.5 M sodium acetate solution. It

was then ejected (50% duty cycle for 10 min, -10 µA) after the next positive effect was obtained. The following day, a multibarrel containing only bicuculline or gabazine was lowered into the same site. A single 90 min ejection was made with a current intensity of 100 nA. At the end of this ejection, the animal was removed from the restraining frame and perfused. As controls, other animals received 90 min injection of NaCl 0.9% with a current intensity of 100-200 nA before perfusion.

Unit recordings and micropharmacology.

Extracellular recordings from individual SLD neurones were obtained with glass microelectrodes (10-20 MΩ, impedance measured at 10 Hz) filled with sodium acetate (0.5M) containing 2% (w/v) of PSB and connected to a preamplifier (P16, Grass). Single unit activity was visualized (signal-to-noise ratio of at least 3:1) on a digital storage oscilloscope (2211 Tektronix) as filtered (AC, band-pass 0.3-10 kHz) and unfiltered signals (DC). The AC trace was used for the on-line count of action potentials with an amplitude-sensitive spike discriminator (Neurolog Spike Trigger, Digitimer Ltd., UK) whose output was also monitored through a speaker driven by an audio amplifier (AM8, Grass). The unfiltered signal was used for on-line identification of the recorded neurones (spike shape and duration). Discriminator output pulses, analog signals proportional to the magnitudes of iontophoretic currents as well as EEG and EMG recordings were collected on a computer via a CED interface using the Spike 2 software (Cambridge Electronic Design, UK). For an additional set of neurones, SLD single unit recording was combined with microiontophoresis. In this case, a four-barrels micropipette (10-15 µm tip diameter) was glued alongside the recording micropipette as described previously (Akaoka et al., 1992, Gervasoni et al., 2000) and filled with carbachol, kainic acid, gabazine and NaCl.

Neuroanatomical experiments

The experimental protocol of the tract-tracing methods has been described in detail in our previous papers (Luppi et al., 1990, 1995; Peyron et al., 1996, 1998). Nine to fifteen days after the CTb injection, the animals were perfused with a Ringer's lactate solution containing 0.1% heparine, followed by 500 ml of a fixative composed of 4% paraformaldehyde and 0.2% picric acid in 0.1M phosphate buffer (PB, pH 7.4). The brains were postfixed 2 hours in the same fixative at 4°C. They were then stored at 4°C for at least two days in 30% sucrose in 0.1M PB. Then, the brains were rapidly frozen with CO_2 gas. Coronal sections (25µm) were obtained with a cryostat and stored in 0.1 M PB, pH 7.4 containing 0.9% NaCl, 0.3% Triton X-100 (PBST) and 0.1% sodium azide (PBST-Az).

The free-floating sections were then successively incubated in: (1) a goat antiserum to CTb (1:40,000; List Biological Lab.), a rabbit antiserum to PHA-L (DAKO, 1:5,000) or a rabbit antiserum to C-Fos (1:5,000, Oncogene, USA) in PBST-Az over 3-4 days at 4°C; (2) a biotinylated rabbit anti-goat or goat anti-rabbit IgG (1:2,000; Vector Laboratories, Burlingame, CA) for 90 min at room temperature; and (3) a ABC-HRP solution (1:1,000; Elite kit, Vector Labs.) for 90 min at room temperature. Then, the sections were immersed in a 0.05 M Tris-HCl buffer (pH 7.6) containing 0.025% 3,3'-diaminobenzidine-4 HCl (DAB; Sigma), 0.003% H_2O_2 and 0.6% nickel ammonium sulfate for 15 min at room temperature. The reaction was stopped by two rinses in PBST-Az. In single staining experiments, the sections were then counterstained with neutral red, mounted on gelatin-coated slides, dried, dehydrated and coverslipped with Depex.

In double immunostaining experiments, PHA-L or C-Fos stained sections were further successively incubated in (1) a rabbit antiserum to glycine (1:10,000, courtesy of D. Pow, Australia), a rabbit antiserum to C-Fos (1:5,000, Oncogene, USA) or a goat antiserum to choline-acetyltransferase (1:2,500, Chemicon, USA) in PBST-Az over 3-4 days at 4°C; (2) a biotinylated donkey anti-rabbit IgG or rabbit anti-goat IgG (1:1,000; Vector Labs.); and (3) ABC-HRP (1:1,000; Elite kit, Vector Labs.) both for 90 min at room temperature. Finally, the sections were immersed

for 15 min at room temperature in the same DAB solution as above without nickel. All incubations and rinses were made in PBST-Az except for the DAB.

Data analysis

Analysis of iontophoretic applications

The polygraphic recordings before, during and after the ejections were analyzed off-line by visual assessment of the EMG, EEG, EOG traces and EEG spectrum during 10-s epochs. These epochs were scored as W, SWS, PS or PS-like using the following criteria. W was characterized by desynchronized (or activated) low amplitude EEG accompanied by a sustained EMG activity with phasic bursts (twitches). SWS was clearly distinguished by high voltage slow waves and spindles and disappearance of phasic muscular activity in an animal immobile and eyes closed. A decrease in the EEG amplitude characterized by a pronounced theta rhythm associated with a flat EMG (i.e. muscle atonia) signaled the onset of PS episodes. Long periods characterized by a flat EMG associated with a desynchronized low amplitude EEG with or without theta activity obtained following kainic acid, bicuculline or gabazine iontophoresis were scored as PS-like periods. The hypnogram was drawn directly in a special channel of the Spike 2 recorded file using a script designed for this purpose.

For each ejection, the absolute value of the EMG (rectified amplitude) was computed and then exported from Spike 2 file for periods of 5 seconds of control W, SWS, PS and for one hour from the beginning of the ejection. The mean and standard deviation of the rectified value of the EMG was then calculated for control PS from 10 extracted values. The onset of the effect (latency, s) was defined as the time interval between the onset of the bicuculline, gabazine or kainic acid application and the moment at which the mean rectified value of the EMG reached a value inferior to the mean control PS value plus one standard deviation. The recovery time was defined as the time-interval between the offset of the ejection and the moment at which the mean rectified value of

the EMG had returned to a stationary level superior to the mean control PS value plus one standard deviation. The duration of the effect corresponds to the period between its onset and its offset.

EEG frequency band activities were computed using a Spike 2 script executing a fast Fourier transform on 5 s EEG epochs with 512 points corresponding to a resolution of 0.4 Hz. All values were then exported from Spike 2 to Microsoft Excel. A seven point smoothing window was first applied to the values. The sum of all values in each frequency band was then calculated. Frequency bands were defined as: delta (1.6-4 Hz), theta (4.4-8.8 Hz), sigma (9.2-14.4 Hz), beta 1 (15.2-19.2 Hz), beta 2 (19.6-31.2 Hz) and gamma (31.6-47.6 Hz, eliminating frequency >47.6 Hz to avoid any possible contamination from AC noise). The ratio of theta/delta was also calculated. To establish the nature of the effects and illustrate them, figures showing delta, theta, sigma, gamma, theta/delta ratio, muscle activity and the hypnogram before, during and after the drug application were generated using Microsoft Excel scripts.

For statistical analysis, the average of 10 absolutes values of the EMG taken during control W, SWS, PS and the effect was calculated for each ejection. The values corresponding to the ejections were taken 300s after the beginning of the effect. For EEG analysis, the mean of 10 relative values taken at the same time that the EMG values was calculated for each band of the EEG (delta, theta, sigma, beta 1, beta 2 and gamma) and the theta/delta ratio. Then, mean±SEM of these values were computed and one-way analyses of variance (ANOVAs) followed by post hoc comparisons were performed (Table 1).

Unit activity analysis

The firing rate of SLD neurones was analyzed off-line using Spike 2 software. All spike counts were taken from computer records of integrated impulse activity (1 s bin width). Firing rates of each recorded cell during W, SWS and PS were extracted from 50 s period of each state using

polygraphic criteria and EEG spectral analysis. Then, means and SEMs deviations of the firing rates were determined and a one-way analysis of variance (ANOVA) followed by post hoc comparisons was performed.

Analysis of neuroanatomical results

Drawings of double-immunostained sections (C-Fos/gly, PHA-L/C-Fos) were made with a Leitz Orthoplan microscope equipped with an X/Y sensitive stage and a video camera connected to a computerized image analysis system (Historag, BIOCOM, France). To precisely determine the location and number of C-Fos and C-Fos/gly stained neurones following 90 min bicuculline, gabazine or NaCl injections immediately before perfusion, we bilaterally plotted and counted in three experimental and three control rats on 10 sections from the hypothalamus to the medulla oblongata C-Fos labelled cells in the major efferents of the SLD. C-Fos and C-Fos/gly labelled cells were counted on four medullary sections in these rats. Then, the mean±SEM numbers of C-Fos and C-Fos/gly labelled cells were determined and a one-way analysis of variance (ANOVA) and post hoc comparisons was performed (Table 2).

In one animal, the PHA-L anterogradely-labelled fibers were drawn, C-Fos labelled neurones were plotted and neuronal structures were delineated from preoptic to medullary levels on double-immunostained sections. C-Fos labelled neurones were first plotted and neuronal structures were delineated from preoptic to medullary levels using Historag. PHA-L labelled fibers visualized on the same sections were then drawn with a pencil separately with the camera lucida technique. The drawn fibers were then scanned and superimposed with that of the C-Fos labelled neurones and the neuronal structures using Adobe illustrator 9. Then, the number of labelled fibers in each efferent structure of the SLD was counted using a fixed window of 500x300µm. In the text, we used the term large number of fibers when the number of fibers counted was superior to 40,

13

substantial when the number was between 40 and 20, small for a number between 20 and 8 and a few for a number between 8 and 1.

Results

Effect of bicuculline, gabazine or carbachol microiontophoresis into the SLD

A state resembling PS was produced in close temporal association of 15 min ejections of bicuculline (n= 24, 12 rats) or gabazine (n=4, 2 rats) in the SLD. It was characterized by a muscle tone similar to that seen during spontaneous PS episodes and significantly inferior to that seen during control W and SWS (p<0.001) (Fig. 1-3, Table 1). The PS-like state appeared 4.3±0.5 min or 7.9±2.5 (mean±SEM) after the onset of bicuculline or gabazine ejections, respectively (Figs. 1-3). The PS-like state remained present during the entire ejection period and terminated 18.9±1.3 and 30.8±6.9 min after its onset respectively. The gabazine effect appeared significantly later and lasted longer than that of bicuculline (p>0.05). No reaction to visual (shaking hands in front of the rat) or auditory (snaps) stimuli was evocable during this period. In all rats in which an electrooculogram was recorded (n=11), no or only a few ocular movements were observed during the PS-like state (Fig. 1). In rats in which erections were simultaneously monitored (n=3), erectile events were rarely seen during this period (Fig.1). We found a mean of 14.7±1.8 erections per hour of spontaneous PS while in the head-restrained apparatus, but only 1.8±1.2 erections per hour during the PS-like state.

In a first group of bicuculline (n=9) and (n=2) gabazine ejections, the muscle atonia was accompanied by an EEG intermediate between PS and W (Table 1). It was characterized by a theta activity significantly superior to that seen during spontaneous W and SWS and inferior to that seen during natural PS (p<0.001) (Figs. 1-3). The delta activity was significantly inferior to that seen during control SWS (p<0.001) while the gamma activity was similar to that seen during control PS and significantly superior to that of W (p<0.001).

In a second group of bicuculline (n=15) and gabazine (n=2) ejections, the muscle atonia was accompanied by a low voltage fast EEG (Fig. 3). Detailed EEG spectral analysis revealed that the

different EEG bands were comparable in power to that seen during spontaneous W and statistically different from those observed during natural SWS or PS (Table 1).

Fifteen minutes iontophoretic ejections of carbachol (n=9, 5 rats) were made from an adjacent barrel of the multibarrel pipette assembly into the sites where a PS-like state was induced by bicuculline or gabazine. Carbachol produced a state similar to W characterized by an increased muscle tone with or without phasic activity and an EEG close to that seen during W and significantly different from that seen during SWS and PS (Fig. 4, Table 1). The bicuculline ejection site successful in generating a PS-like state was highly restricted for each rat. Deviation from the effective site (n=14, 8 rats) by only 0.5-1.0 mm ventro-dorsal, medio-lateral or rostro-caudal from a positive site obtained with the same multibarrel assembly produced a state indistinguishable from W, characterized by low delta, sigma and theta activities and a tonic muscle activity with or without active body movements.

Following 15 minutes ejection of NaCl (15 min, 100-200 nA) (n=4, 4 rats), no change in the muscle tone or sleep-wake architecture was seen.

Eight rats were administered a continuous injection of bicuculline or gabazine into the SLD to determine whether the PS-like state could be maintained throughout the duration of this ejection period and induce C-Fos expression. Ejections of bicuculline (n=6) or gabazine (n=2) for 90 min induced a PS-like state with a latency of 2.38 ± 1.0 or 6.9 ± 2.1 min, respectively. This PS-like state continued throughout the 90 min ejection period of bicuculline or gabazine for 86.9 ± 3.4 min or 75.5 ± 11.0 min, respectively (Fig. 5). For all rats, the muscle tone was similar to that seen during control PS episodes and statistically inferior from that occurring during W and SWS ($p<0.0???$, Table 1). In four rats, the EEG power spectrum was intermediate between PS and W (Table 1, SP-like with theta) and in four other rats it was close to that of W and significantly different from PS and SWS (Table 1, SP-like without theta).

The rats which received a saline (100-200 nA) (n=4) ejection in the SLD during 90 min, showed no decrease in muscle tone. They spent 45.4±12.7 min in W, 33.5±11.7 min in SWS and 6.9±2.5 min in PS.

Effect of bicuculline and kynurenic acid co-administration

The iontophoretic administration of bicuculline (100nA) into the SLD in this set of experiments (n=6, 4 rats) also induced a PS-like state with a latency of 4.9±0.9 min characterized by an EMG similar to that seen during control PS episodes and statistically inferior to that seen during control SWS and W (Table 1). The EEG power activity was either intermediate between that seen during PS and W (n=4) or similar to that of W (n=2) (Table 1). At least 5 min after the beginning of the bicuculline effect, kynurenic acid (100 nA) was co-administered from an adjacent barrel for 3 to 10 min (Fig. 6). Following kynurenic acid application, the EMG muscle tone increased and reached a value similar to that seen during W and statistically superior to that seen during PS (p<0.001) with a latency and duration of 2.3±0.9 min and 7.0±0.8 min, respectively. When the ejection of kynurenic acid was stopped, the EMG returned to the previous muscle atonia with an amplitude similar to that seen during control PS episodes (Fig. 7). During the increase of muscle tone induced by kynurenic acid co-administration, no significant change in the EEG pattern was observed compared to bicuculline alone (Table 1).

Effect of kainic acid microiontophoresis in the SLD

Iontophoretic application of kainic acid (100 nA) in the SLD (n=5, 3 rats) for 5 min induced a PS-like state characterized by a complete disappearance of the muscle tone within 2.1±0.7 min for

a duration of 9.3±1.2 min (Fig. 7, Table 1). The muscle atonia was associated with an activation of the EEG. The delta, theta, and sigma activities during the kainic acid effect were similar to those seen during control W and statistically different from that of PS and SWS (p<0.0???, Table 1). The PS-like state obtained with kainic acid was followed in all cases by a large increase in muscle tone associated with active movements of the extremities and a low voltage EEG activity resembling wakefulness for a duration of 62.2±28.56 min.

Recordings of SLD neurones across the sleep-waking cycle with simultaneous iontophoretic administration of carbachol, kainic acid or gabazine.

Nine neurones with an activity specific to PS were recorded in the SLD in four rats. They had a discharge rate significantly superior during PS (21.7±1.7 Hz) than during SWS (1.1 ±0.2 Hz) and W (0.7 ± 0.1 Hz)(p<0.001). These neurones started firing slightly before the onset of PS and stopped firing just before its offset (Fig. 8). On three SLD neurones, carbachol, kainic acid or gabazine were iontophoretically applied. Application of kainic acid (50 nA) for 3-5 s induced a substantial increase in their discharge rates (Fig. 9A), whereas the application of carbachol (50 nA) for 30 s induced no effect (Fig. 9B). Long lasting application of gabazine (100 nA) induced a strong activation of the recorded neurones and the onset of a PS-like episode (Fig. 9A). To ensure that carbachol was ejected in our protocol, we iontophoretically applied carbachol on neurones recorded during the descent to the SLD region. Carbachol iontophoresis dorsal to the SLD induced either an increase or a decrease in neuronal discharge (data not shown).

Localization of the injection sites

The bicuculline, gabazine or kainic acid positive injection sites were determined by mean of CTb, PHA-L, PSB or C-Fos staining. For all injections that induced a complete muscle atonia with an EEG close to W or intermediate between W and PS, the sites were intermingled in or adjacent to

the SLD (Figs. 10A,B, 11) as defined by Swanson (1992). The majority of the sites (n=9) were restricted to the portion of this nucleus just rostral to the motor trigeminal nucleus (V) (Figs.10B, 11B). A smaller number of positive sites (n=7) was localized in the SLD region at the level of the rostral portion of the V (Figs. 10A, 11C,D).

The CTb, PHA-L or PSB injection sites localized in the pontine periaqueductal gray (PAG) region encompassing the rostral pole of the LC, Barrington nucleus, and MEV (Fig. 11C,D) or in the caudal pontine reticular nucleus medial to the V, the medial parabrachial nucleus (PBm) or the rostral pontine reticular nucleus, corresponded to ejections that induced W characterized by an increase in muscle activity and an activated EEG.

The distribution of C-Fos-labelled neurones in the injection site was studied in animals that received a 90 min ejection of bicuculline (n=6) or gabazine (n=2) immediately prior to transcardial perfusion, as well as in NaCl control (n= 4) ejected animals. In the case of bicuculline or gabazine ejections that induced a 90 min sustained period of a PS-like state, a large number of C-Fos labelled neurones was localized in the SLD and the adjacent ventral LDT, dorsal pontine reticular and PPN nuclei within a radius of 350-500μm around the injection point (Fig. 12A, Table 2). On sections double-stained with choline acetyl transferase (ChAT) and C-Fos, only occasional (1-2 per section) C-Fos/ChAT neurones were observed in the SLD and LDT. In control animals injected with NaCl, only a few C-Fos labelled neurones were seen in the SLD and surrounding nuclei at the same level (Table 2).

Projections of the SLD
Anterograde tracing

Following PHA-L or CTb injections restricted to the SLD in which a positive effect was obtained, the anterograde labelling obtained was bilateral with a slight ipsilateral predominance.

A large bundle of descending fibers was observed in the dorso-lateral part of the caudal pontine reticular nucleus medial to the V. The bundle extended caudally ventral to the genu of the

facial nerve and then terminated dorso-medially to the rostral facial motor nucleus. At the medullary level, a large number of anterogradely labelled varicose fibers was observed in the gigantocellular reticular (GRN), magnocellular reticular (MARN) (Fig. 12C,D) and parvicellular reticular (PARN) nuclei (Fig. 13D). A substantial number of varicose fibers was also localized in the raphe magnus (RM), parvicellular reticular alpha (PARNA), and dorsal and lateral paragigantocellular reticular nuclei (PGRNd, PGRNl) (Fig. 13C,D).

At the level of the site of injection, a large number of varicose fibers was seen in the contralateral SLD and in the caudal pontine reticular nucleus (PRNc). Slightly rostral to the sites, a very large number of fibers was localized in the PRNr region ventrolateral to the caudal ventral tegmental nucleus of Gudden. At this level and more rostrally, a substantial number of varicose fibers was diffusely distributed bilaterally in the other parts of the PRNr and to a lesser extent the LDT and the lateral parabrachial nucleus (PBl). A small number of fibers was distributed in the median raphe nucleus.

A bundle of ascending fibers was clustered in the dorsal tegmental bundle (dtg) all along its rostro-caudal extension. All along its path, the bundle left a large number of varicose fibers in the mesencephalic reticular nucleus (MRN) caudally and also more rostrally in the caudal interstitial nucleus. At this level, a substantial number of varicose fibers was localized in the ventrolateral PAG and to a lesser extent the dorsal raphe nucleus. A small number of fibers was seen in the red nucleus. The bundle ended in the rostral part of the interstitial and parafascicular thalamic nuclei in which a large number varicose fibers was observed. More rostrally, a large number of passing and varicose fibers was seen in the zona incerta (ZI). A substantial number of varicose fibers was seen in the lateral hypothalamic area and the perifornical nucleus. At this level, a large number of varicose fibers was localized in the central medial, paracentral and centrolateral thalamic nuclei. Finally, a small number of fibers was seen in the lateral preoptic area and the nucleus of the horizontal limb of the diagonal band.

Distribution of C-Fos labelled cells

The distribution of C-Fos-labelled neurones in the main SLD efferents was studied in three animals that received a continuous ejection of bicuculline or gabazine for 90 min immediately prior to perfusion and in three control NaCl ejected animals.

At the caudal pontine and medullary level, the PARN, PARNA, MARN, cRM and PGRNl contained a substantial to large number of C-Fos labelled cells. The labelling was bilateral for the cRM, PGRNl and PARN and predominantly ipsilateral for the PARNA and MARN (Table 2, Fig. 13 C,D). In control animals, only occasional C-Fos labelled cells were observed in these structures (Table 2). The difference in number of cells between drug and control condition reached statistical significance for the PARN, MARN and PGRNl ($p < 0.0???$, Table 2). Following drug application, a small number of C-Fos labelled cells statistically superior to control condition was also localized in the PGRNd and the GRN (Table 2).

In the major rostral efferents of the SLD, a substantial to large number of neurones was seen in the ventrolateral PAG, MRN, parafascicular thalamic nucleus (PF), ZI, lateral hypothalamic area and the intralaminar thalamic nuclei in drug treated animals (Fig. 13A). The number of cells in these structures was generally higher compared to control conditions (Table 2) but it reached statistical significance only for the intralaminar thalamic nuclei.

Localization of the glycinergic neurones activated during PS

In order to identify the glycinergic neurones responsible for the muscular atonia during PS, C-Fos/gly and PHA-L/gly immunohistochemistry were combined.

On PHA-L/gly double-labelled sections, a large number of PHA-L varicose fibers was seen in close vicinity to glycine-immunoreactive neurones in the ipsilateral MARN (Fig. 12D,E), cRM and bilaterally in the PARN and PARNA.

On C-Fos/gly double-immunostained sections from rats injected with bicuculline or gabazine for 90min before perfusion, a substantial number of double-labelled neurones was seen with an ipsilateral predominance in the PRNc, MARN, and bilaterally in the cRM (Fig. 12B), PGRNl and PARN (Fig. 14)(Table 2). In addition, in these animals, a small number of double-labelled cells was seen in the PARNA, and PGRNd. In control condition, no or occasional cells were seen in these nuclei. The difference between drug and control conditions was statistically significant for the MARN, PGRNl, PARN and PGRNd ($p<0.0???$, Table 2).

Discussion

We demonstrate for the first time that a long-lasting PS-like hypersomnia can be pharmacologically induced with a short latency in rats by iontophoretically administering bicuculline, gabazine or kainic acid specifically into the SLD. Carbachol, however, was not effective in this regard. We also showed that the bicuculline effect can be reversed by the application of kynurenic acid, and we recorded neurones in the SLD that are specifically active during PS. We further demonstrated that ventromedial and lateral medullary reticular structures receive a strong projection from the SLD. A neuroanatomical analysis of these medullary neurones revealed numerous C-Fos and glycine double-stained neurones following long application of bicuculline or gabazine in the SLD. These results suggest that PS executive neurones localized in the SLD in the rat play a role in PS generation and the maintenance of muscle atonia through the following mechanisms : 1) They are tonically inhibited by GABA during waking and slow wave sleep; 2) They receive a tonic glutamatergic input during all states of vigilance; and 3) They directly project to intralaminar thalamic neurones and glycinergic neurones localized in the ventromedial and lateral medullary reticular formation.

There are numerous differences between rats and cats regarding the effectiveness of carbachol administration into the pontine reticular formation, and most studies have had limited success replicating the strong PS hypersomnia obtained in cats (Baghdoyan et al., 1987; Vanni-Mercier et al., 1989; Lai and Siegel, 1990; Yamamoto et al., 1990; Garzon et al., 1998). The enhancement of PS in rats was of small magnitude (Gnadt and Pegram, 1986; Shiromani and Fishbein, 1986; Velazquez-Motezuma et al., 1989; Bourgin et al., 1995) or not reliably obtained (Deurveilher et al., 1997). The increase in PS, when obtained, was less than 100% compared to the 300% increase obtained in cats. In addition, the first PS episode appeared at least 50 min after the carbachol injection and the duration of the episodes were similar to natural, spontaneous, PS. In cats, however, PS is induced almost immediately after the injection and the episodes last longer

than in control PS. The effective sites in rats were widely distributed in the pontine reticular formation including the PRNr, PRNc and the SLD. In contrast, the effective sites in cats were either localized just ventral to the locus coeruleus alpha nucleus in an area called peri-LCα by Sakai et al. (1979, 1981) or in the ventral part of the PRNr (Garzon et al., 1998). In our experiments, carbachol applications were unable to induce a PS-like state when applied to the dorsal parts of the PRNr, PRNc or the SLD. Instead carbachol induced a W state with an increased muscle tone. Moreover, PS-on neurones recorded in the SLD were not excited or inhibited by carbachol iontophoresis, in contrast to PS-on neurones recorded in cats in the peri-LCα (Sakai and Koyama, 1996; Koyama and Sakai, 2000). This result is not due to a technical difficulty since iontophoretic applications with the same multibarrel during the same descent induced either an excitation or an inhibition of neuronal discharge dorsal to the SLD.

Our results suggest a strong species difference between rats and cats. The absence of an effect of carbachol does not rule out a cholinergic mechanism in PS onset and maintenance in the rat. Nevertheless, it suggests that cholinergic input to SLD neurones plays at most a minor role in their regulation in this species. It remains to be determined whether the cholinergic system plays an important role in PS control in rats via a different population of neurones located in another pontine region. Another possibility is that PS-on neurones in the SLD region express muscarinic and/or nicotinic receptors, but that the activation of these receptors by carbachol is unable to modify their activity. This could be due to the strong GABAergic tonic inhibition revealed by our results. Indeed, microiontophoresis of bicuculline or gabazine, two different $GABA_A$ antagonists, in the SLD region induced a state closed to PS. These data rule out the possibility that the sustained PS-like state is due to a non-specific neuronal activation by bicuculline, as previously suggested under different experimental conditions (Debarbieux et al., 1998). It strongly suggests that GABA tonically inhibits PS-on neurones localized in the SLD during W and SWS. Our results are in agreement with a recent study in cats showing that pressure application of bicuculline in the peri-

LCα region induces a strong increase in PS quantities with short latencies, whereas the application of GABA strongly decreases PS (Xi et al., 1999).

We also showed that iontophoretic kainic acid application into the SLD induced an activation of PS-on neurones and is consistently associated with a transient PS-like state followed by W and an increase in muscle activity. In agreement with our results, it has been shown in cats that the administration of kainic acid in the peri-LCα using microdialysis induces a PS-like state (Onoe and Sakai, 1995). Finally, we showed that the application of kynurenic acid, an excitatory amino acid antagonist, reversed the PS-like state induced by bicuculline application in the SLD. Altogether, these results suggest that PS-on neurones in the SLD region receive a tonic glutamatergic input during all sleep-waking states.

Altogether, these data imply that the onset of PS, at least in rats, is mainly due to the removal of a tonic GABAergic input present during W and SWS. The GABAergic neurones responsible for this tonic inhibition could be interneurones or long projection neurones. Indeed, GABAergic interneurones have been localized in the SLD (Ford et al., 1995) and GABAergic neurones with long projections to brainstem nuclei have been identified as well (Gervasoni et al., 2000).

In the dorsal pontine reticular formation, neurones responsible for PS onset and maintenance seem to be clustered in the SLD. Indeed, injections just 500 µm away from the positive sites induced W with an increased muscle activity. Moreover, C-Fos labelled neurones in the site of injection following long bicuculline applications occupied less than 1mm^3. The neurochemical nature of the neurones in the SLD remains to be determined. It is unlikely that they are cholinergic since we showed that the great majority of the C-Fos positive neurones in the injection site were not immunoreactive to ChAT. One likely possibility is that these neurones are glutamatergic neurones since our C-Fos experiments highly suggest that they provide an excitatory pathway to glycinergic neurones in the medullary reticular formation. Additional studies are necessary to test this hypothesis.

Bicuculline or gabazine administration into the SLD induced a PS-like state characterized by the presence of muscle atonia, EEG activation with or without theta activity, and non-reactivity to surrounding stimuli, but the absence of ocular movements or penile erections. The absence of rapid eye movements and penile erections may be due to the fact that our injections were only unilateral. Indeed, bilateral activation of SLD neurones may be necessary to obtain all phenomena characteristic of PS. Another possibility is that the SLD neurones are not responsible for all PS-related phenomena. Cholinergic and non-cholinergic neurones from the LDT or neurones from other structures could be responsible for the missing tonic or phasic events. Supporting this hypothesis, neurones specifically active during PS-related erections have been recently recorded in the LDT (Koyama et al., 2001). Moreover, an increased number of C-Fos positive neurones has been observed in the LDT following PS rebound (Maloney et al., 1999). In our experiments, bicuculline injections into the LDT induce W in apparent contradiction with this hypothesis. This finding may be explained by the fact that the majority of the LDT neurones exhibit a high firing rate both during W and PS, whereas only a minority are specifically active during PS (El Mansari et al., 1989; Steriade et al., 1990).

In our study, we also attempted to determine the neuronal network responsible for the cortical activation and the muscle atonia seen following bicuculline, gabazine or kainic acid applications in the SLD.

Concerning the muscle atonia, we demonstrate that numerous glycine-immunoreactive neurones contain C-Fos in the cRM, MARN, PARN and PARNA following bicuculline or gabazine applications in the SLD region. It is likely that that at least some of these glycinergic neurones are responsible for the muscle atonia seen during PS. Indeed, intracellular recordings of motoneurones combined with strychnine applications show that glycine is responsible for the tonic hyperpolarization of the spinal, hypoglossal and trigeminal motoneurones during PS (Chase et al., 1989; Soja et al, 1991; Kohlmeier et al., 1996; Yamuy et al., 1999). It has also been shown that glycinergic neurones from the MARN directly project to spinal motoneurones (Holstege et al.,

1991) while glycinergic neurones from the PARN and PARNA directly project to the trigeminal motor nucleus (Li et al., 1996; Rampon et al., 1996). Moreover, it has been shown in cats following induction of PS by carbachol injections in the peri-LCα that cells in the MARN labelled with C-Fos project to the V (Morales et al., 1999). Altogether, these and our results indicate that glycinergic neurones from the MARN, PARN and PARNA could be responsible for the hyperpolarization of spinal and cranial motoneurones during PS.

The hypothesis suggesting that glycinergic neurones from the PARN, RM and MARN are involved in the generation of muscle atonia is also supported by our finding of a strong projection from the SLD to these nuclei. Indeed, previous studies in cats demonstrate a strong projection from the peri-LCα to the magnocellular reticular nucleus (Sakai et al., 1979; Luppi et al., 1988). In contrast, only a minor projection from the peri-LCα to the PARN has been described (Fort et al., 1994). The apparent discrepancy between this and our study might be due to the fact that the strongest projection from the SLD to the PARN innervates the caudal and lateral parts of the nucleus, a region not studied in the previous study.

In addition to descending projections to the medullary reticular formation, we also found that the SLD region projects to rostral structures like the intralaminar thalamic nuclei, intrafascicular thalamic nucleus and zona incerta, in agreement with Jones and Yang (1985). The ascending projection to the intralaminar thalamic nuclei could be responsible for the cortical activation obtained during the administration of bicuculline, gabazine or kainic acid into the SLD since numerous C-Fos labelled neurones were localized in these nuclei following long lasting bicuculline or gabazine ejections into the SLD.

Conclusions

In the present study, we localize for the first time in rats a pontine PS-inducing region similar to that previously found in cats. We further provide strong evidence that PS-on neurones in

the SLD are tonically inhibited by GABA during W and SWS, under constant glutamatergic control and unresponsive to carbachol. Using anterograde tracing with PHA-L combined with C-Fos and glycine immunohistochemistry, we further showed that the SLD neurones provide an excitatory projection to glycinergic neurones from the ventromedial and lateral medullary reticular formation. From these results, we propose that the onset and maintenance of PS could be due to the activation of PS-on neurones localized in the SLD. The activation of these neurones would primarily be due to the removal of a tonic GABAergic inhibitory input present during W and SWS in combination with a constant tonic glutamatergic input. Further studies are now necessary to test this new hypothesis.

Acknowledgments

Abbreviations

ChAT: choline acetyltransferase

cRM: caudal nucleus raphe magnus

CSP: corpus spongiosum of the penis

CTb: cholera-toxin B subunit

DAB: 3,3'-diaminobenzidine-4 HCl

dtg : dorsal tegmental bundle

EEG: electroencephalogram

EMG: electromyogram

EOG: electrooculogram

gly: glycine

GRN: gigantocellular reticular nucleus

ILM: intralaminar nuclei of the dorsal thalamus

LC: locus coeruleus nucleus

LDT: laterodorsal tegmental nucleus

MARN: magnocellular reticular nucleus

MEV: mesencephalic nucleus of the trigeminal

MRN: mesencephalic reticular nucleus

PAG: periaqueductal gray

PARN: parvicellular reticular nucleus

PARNA: parvicellular reticular nucleus alpha

PB: phosphate buffer

PBl: lateral parabrachial nucleus

PBm: medial parabrachial nucleus

PBST: phosphate buffer saline Triton X

PBST-Az: phosphate buffer saline Triton X azide

peri-LCα: peri-locus coeruleus α

PF: parafascicular thalamic nucleus

PGRNd: dorsal paragigantocellular reticular nucleus

PGRNl: lateral paragigantocellular reticular nucleus

PHA-L: phaseolus leucoaglutinin

PPN: pedunculopontine nucleus

PRNc: caudal pontine reticular nucleus

PRNr: rostral pontine reticular nucleus

PS: paradoxical sleep

PSB: pontamine sky blue

REM: rapid eye movement sleep

RM: nucleus raphe magnus

SWS: slow wave sleep

W: waking

ZI: zona incerta

References

Akaoka, H., Charlety, P.J., Saunier, C.F., Buda, M. & Chouvet, G. (1992) Combining *in vivo* volume-controlled pressure microinjection with extracellular unit recording. *J. Neurosci. Methods*, **42**, 119-129.

Aserinsky, E. & Kleitman, N. (1953) Regularly occurring periods of eye motility and concomitant phenomena during sleep. *Science*, **118**, 273-274.

Baghdoyan, H.A., Rodrigo-Angulo, M.L., McCarley, R.W. & Hobson, J.A. (1987) A neuroanatomical gradient in the pontine tegmentum for the cholinoceptive induction of desynchronized sleep signs. *Brain Res.*, **414**, 245-261.

Bourgin, P., Escourrou, P., Gaultier, C. & Adrien, J. (1995) Induction of rapid eye movement sleep by carbachol infusion into the pontine reticular formation in the rat. *NeuroReport*, **6**, 532-536.

Chase, M.H., Soja, P.J. & Morales, F.R. (1989) Evidence that glycine mediates the postsynaptic potentials that inhibit lumbar motoneurons during the atonia of active sleep. *J. Neurosci.*, **9**, 743-751.

Darracq, L., Gervasoni, D., Soulière, F., Lin, J.S., Fort, P., Chouvet, G. & Luppi, P.H (1996) Effect of strychnine on rat locus coeruleus neurons during sleep and wakefulness. *NeuroReport*, **8**, 351-355.

Debarbieux, F., Brunton, J. & Charpak, S. (1998) Effect of bicuculline on thalamic activity: a direct blockade of IAHP in reticularis neurons. *J. Neurophysiol.*, **79**, 2911-2918.

Dement, W. & Kleitman, N. (1957) Cyclic variations of EEG during sleep and their relation to eye movement., body motility., and dreaming. *Electroenceph. Clin. Neurophysiol.*, **9**, 673-690.

Dement, W. (1958) The occurrence of low voltage., fast., electroencephalogram patterns during behavioral sleep in the cat. *Electroenceph. Clin. Neurophysiol.*, **10**, 291-296.

Deurveilher, S., Hars, B. & Hennevin, E. (1997) Pontine microinjection of carbachol does not reliably enhance paradoxical sleep in rats. *Sleep*, **20**, 593-607.

El Mansari, M., Sakai, K. & Jouvet, M. (1989) Unitary characteristics of presumptive cholinergic tegmental neurons during the sleep-waking cycle in freely moving cats. *Exp. Brain. Res.*, **76**, 519-529.

Ford, B., Holmes, C.J., Mainville, L. & Jones, B.E. (1995) GABAergic neurons in the rat pontomesencephalic tegmentum: codistribution with cholinergic and other tegmental neurons projecting to the posterior lateral hypothalamus. *J. Comp. Neurol.*, **363**, 177-196.

Fort, P., Luppi, P.H., Wenthold, R. & Jouvet, M. (1990) [Glycine immunoreactive neurons in the medulla oblongata in cats] Neurones immunoreactifs à la glycine dans le bulbe rachidien du chat. *C R Acad. Sci. III*, **311**, 205-212.

Fort, P., Luppi, P.H. & Jouvet, M. (1993) Glycine-immunoreactive neurones in the cat brain stem reticular formation. *NeuroReport*, **4**, 1123-1126.

Fort, P., Luppi, P.H. & Jouvet, M. (1994) Afferents to the nucleus reticularis parvicellularis of the cat medulla oblongata: a tract-tracing study with cholera toxin B subunit. *J. Comp. Neurol.*, **342**, 603-618.

Garzôn, M., De Andrés, I. & Reinoso-Suarez, F. (1998) Sleep patterns after carbachol delivery in the ventral oral pontine tegmentum of the cat. *Neuroscience*, **83**, 17-31.

Gervasoni, D., Darracq, L., Fort, P., Soulière, F., Chouvet, G. & Luppi, P.H (1998) Electrophysiological evidence that noradrenergic neurones of the rat locus coeruleus are tonically inhibited by GABA during sleep. *Eur. J. Neurosci.*, **10**, 964-970.

Gervasoni D., Peyron C., Rampon C., Barbagli B., Chouvet G., Urbain N., Fort P. & Luppi PH (2000) Role and Origin of the GABAergic Innervation of Dorsal Raphe Serotonergic Neurons. *J. Neurosci.*, **20**, 4217-4225.

Gnadt, J.W. & Pegram, G.V. (1986) Cholinergic brainstem mechanisms of REM sleep in the rat. *Brain Res.*, **384**, 29-41.

Hobson, J.A., Mc Carley, R.W. & Wyzinski, P. (1975) Sleep cycle oscillation: reciprocal discharge by two brainstem neuronal groups. *Science*, **189**, 55-58.

Holstege, J.C. & Bongers, C.M. (1991) A glycinergic projection from the ventromedial lower brainstem to spinal motoneurons. An ultrastructural double labeling study in rat. *Brain Res.*, **566**, 308-315.

Jones, B.E. & Yang, T.Z. (1985) The efferent projections from the reticular formation and the locus coeruleus studied by anterograde and retrograde axonal transport in the rat. *J. Comp. Neurol.*, **242**, 56-92.

Jones, B.E. (1991) Paradoxical sleep and its chemical/structural substrates in the brain. *Neuroscience*, **40**, 637-56.

Jouvet, M. & Michel, F. (1959) Corrélations électromyographiques du sommeil chez le chat décortiqué et mésencéphalique chronique. *CR Soc. Biol.*, **153**, 422-425.

Kohlmeier, K.A., Lopezrodriguez, F., Liu, R.H., Morales, F.R. & Chase, M.H. (1996) State-dependent phenomena in cat masseter motoneurons. *Brain Res.*, **722**, 30-38.

Koyama, Y. & Sakai, K. (2000) Modulation of presumed cholinergic mesopontine tegmental neurons by acetylcholine and monoamines applied iontophoretically in unanesthetized cats. *Neuroscience*, **96**, 723-733.

Koyama, Y., Schmidt, M.H., Takahashi, K. & Kayama, Y. (2001) Cholinergic neurons in the laterodorsal tegmental nucleus regulate penile erection during paradoxical sleep. *Soc. Neurosci. Abstr.*, **522**.20

Kubin, L. (2001) Carbachol models of REM sleep: Recent developments and new directions. *Arch. Ital. Biol.*, **139**, 147-168.

Lai, Y.Y. & Siegel, J.M. (1990) Cardiovascular and muscle tone changes produced by microinjection of cholinergic and glutamatergic agonists in dorsolateral pons and medial medulla. *Brain Res.*, **514**, 27-36.

Li, Y.Q., Takada, M., Kaneko, T. & Mizuno, N. (1996) GABAergic and glycinergic neurons projecting to the trigeminal motor nucleus: a double labeling study in the rat. *J. Comp. Neurol.*, **373**, 498-510.

Luppi, P.H., Sakai, K., Fort, P., Salvert, D. & Jouvet, M. (1988) The nuclei of origin of monoaminergic., peptidergic., and cholinergic afferents to the cat nucleus reticularis magnocellularis: a double-labeling study with cholera toxin as a retrograde tracer. *J. Comp. Neurol.*, **277**, 1-20.

Luppi, P.H., Fort, P. & Jouvet, M. (1990) Iontophoretic application of unconjugated cholera toxin B subunit CTb combined with immunohistochemistry of neurochemical substances: a method for transmitter identification of retrogradely labeled neurons. *Brain Res.*, **534**, 209-224.

Luppi, P.H., Aston-Jones, G., Akaoka, H., Chouvet, G. & Jouvet, M. (1995) Afferent projections to the rat locus coeruleus demonstrated by retrograde and anterograde tracing with cholera-toxin B subunit and Phaseolus vulgaris leucoagglutinin. *Neuroscience*, **65**, 119-160.

Maloney, K.J., Mainville, L. & Jones, B.E. (1999) Differential c-Fos expression in cholinergic., monoaminergic and GABAergic cell groups of the pontomesencephalic tegmentum after paradoxical sleep deprivation and recovery. *J Neurosci.*, **19**, 3057-3072.

Morales, F.R., Sampogna, S., Yamuy, J. & Chase, M.H. (1999) C-Fos expression in brainstem premotor interneurons during cholinergically induced active sleep in the cat. *J Neurosci*, **19**, 9508-9518

Onoe, H. & Sakai, K. (1995) Kainate receptors : a novel mechanism in paradoxical (REM) sleep generation. *NeuroReport*, **6**, 353-356.

Peyron, C., Luppi, P.H., Fort, P., Rampon, C. & Jouvet, M. (1996) Lower brainstem catecholamine afferents to the rat dorsal raphe nucleus. *J Comp. Neurol.*, **364**, 402-413.

Peyron, C., Petit, J.M., Rampon, C., Jouvet, M. & Luppi, P.H. (1998) Forebrain afferents to the rat dorsal raphe nucleus demonstrated by retrograde and anterograde tracing methods. *Neuroscience* **82**, 443-468.

Rampon, C., Peyron, C., Petit, J.M., Fort, P., Gervasoni, D. & Luppi, P.H (1996) Origin of the glycinergic innervation of the rat trigeminal motor nucleus. *NeuroReport*, **7**, 3081-3085.

Sakai, K., Sastre, J.P., Salvert, D., Touret, M., Tohyama, M. & Jouvet, M. (1979) Tegmentoreticular projections with special reference to the muscular atonia during paradoxical sleep in the cat: an HRP study. *Brain Res.*, **176**, 233-254.

Sakai, K., Sastre, J.P., Kanamori, N. & Jouvet, M. (1981) State-specific neurons in the ponto-medullary reticular formation with special reference to the postural atonia during paradoxical sleep in the cat. In Pompeiano O., Aimone Marsan C (eds): *Brain Mechanisms of Perceptual Awareness and Purposeful Behavior*, Raven Press., New York., pp. 405-429.

Sakai, K. & Koyama, Y. (1996) Are there cholinergic and non-cholinergic paradoxical sleep-on neurons in the pons? *NeuroReport*, **7**, 2449-2453.

Sakai, K., Crochet, S. & Onoe, H. (2001) Pontine structures and mechanisms involved in the generation of paradoxical (REM) sleep. *Arch. Ital. Biol.*, **139**, 93-107.

Schmidt, M.H., Valatx, J.L., Schmidt, H.S., Wauquier, A. & Jouvet, M. (1994) Experimental evidence of penile erections during paradoxical sleep in the rat. *NeuroReport*, **5**, 561-564.

Schmidt, M.H., Valatx, J.L., Sakai, K., Fort, P. & Jouvet, M. (2000) Role of the Lateral Preoptic Area in Sleep-Related Erectile Mechanisms and Sleep Generation in the Rat. *J. Neurosci.*, **20**, 6640-6647.

Shiromani, P.J. & Fishbein, W. (1986) Continuous pontine cholinergic microinfusion via mini-pump induces sustained alterations in rapid eye movement (REM) sleep. *Pharmacol. Biochem. Behav.*, **25**, 1253-1261.

Siegel, J.M. & McGinty, D.J. (1977) Pontine reticular formation neurons: relationship of discharge to motor activity. *Science*, **196**, 678-680.

Soja, P.J., Lopez-Rodriguez, F., Morales, F.R. & Chase, M.H. (1991) The postsynaptic inhibitory control of lumbar motoneurons during the atonia of active sleep: effect of strychnine on motoneuron properties. *J. Neurosci.*, **11**., 2804-2811.

Souliere, F., Urbain, N., Gervasoni, D., Schmitt, P., Guillemort, C., Fort, P., Renaud, B., Luppi, P.H. & Chouvet, G. (2000) Single-unit and polygraphic recordings associated with systemic

or local pharmacology: a multi-purpose stereotaxic approach for the awake., anaesthetic-free., and head-restrained rat. *J. Neurosci. Res.*, **61**, 88-100.

Steriade, M., Datta, S., Paré, D., Oakson, G. & Curro Dossi R.C. (1990) Neuronal activities in brain-stem cholinergic nuclei related to tonic activation processes in thalamocortical systems. *J. Neurosci.*, **10**, 2541-2559.

Stone, T.W. (1985) Microiontophoresis and pressure ejection. In Smith AD (ed): *Methods in the neurosciences*, Wiley, New York.

Swanson, L.W. (1992) *Structure of the rat brain*. Elsevier Science Publishers B.V.

Vanni-Mercier, G., Sakai, K., Lin, J.S. & Jouvet, M. (1989) Mapping of cholinoceptive brainstem structures responsible for the generation of paradoxical sleep in the cat. *Arch. Ital. Biol.*, **127**, 133-164.

Velazquez-Moctezuma, J., Gillin, J.C. & Shiromani, P.J. (1989) Effect of specific Ml., M2 muscarinic receptor agonists on REM sleep generation. *Brain Res.*, **503**, 128-131.

Xi, M.C., Morales, F.R. & Chase, M.H. (1999) Evidence that wakefulness and REM sleep are controlled by a GABAergic pontine mechanism. *J. Neurophysiol.*, **82**, 2015-2019.

Yamamoto, K., Mamelak, A.N., Quattrochi, J.J. & Hobson, J.A. (1990) A cholinoceptive desynchronized sleep induction zone in the anterodorsal pontine tegmentum: locus of the sensitive region. *Neuroscience*, **39**, 279-293.

Yamuy, J., Fung, S.J., Xi, M., Morales, F.R. & Chase, M.H. (1999) Hypoglossal motoneurons are postsynaptically inhibited during carbachol-induced rapid eye movement sleep. *Neuroscience*, **94**, 11-15.

Figure 1:
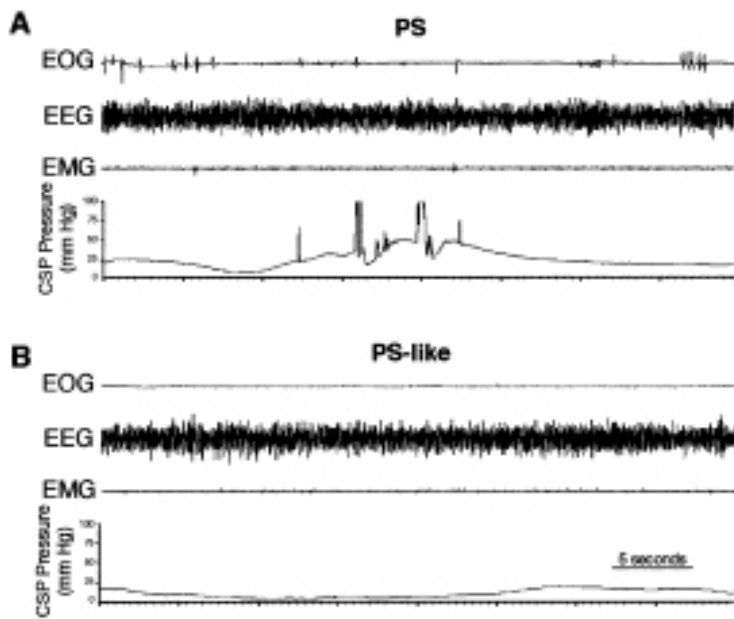
EEG, EOG, pressure within the corpus spongiosum of the penis (CSP) and EMG traces during a control PS episode (A) and during the PS-like state (B) induced by a 15 min bicuculline ejection (100 nA) in the SLD. The penile erection during spontaneous PS is characterized by an increase in baseline CSP pressure from 10-15 mm Hg to a tumescence baseline of 50-70 mm Hg, in addition to brief large CSP pressure peaks (peaks have been truncated so that the lower magnitude pressure can easily be seen). Note the presence during the effect of bicuculline of a theta activity and a muscle atonia similar to that seen during control PS. However, ocular movements and penile erections are absent during this PS-like state.
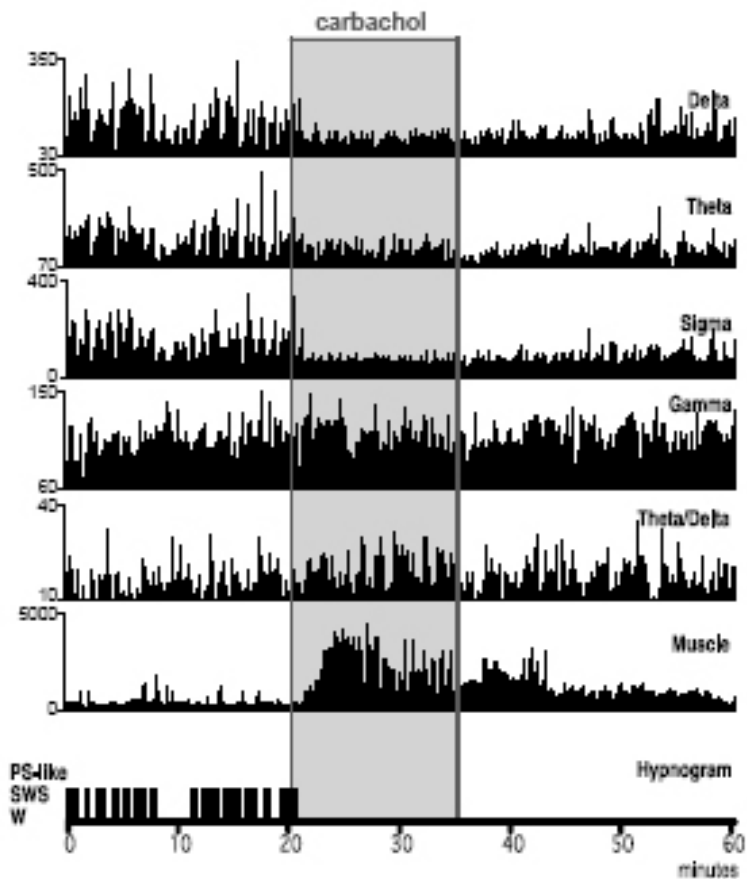
Figure 2:
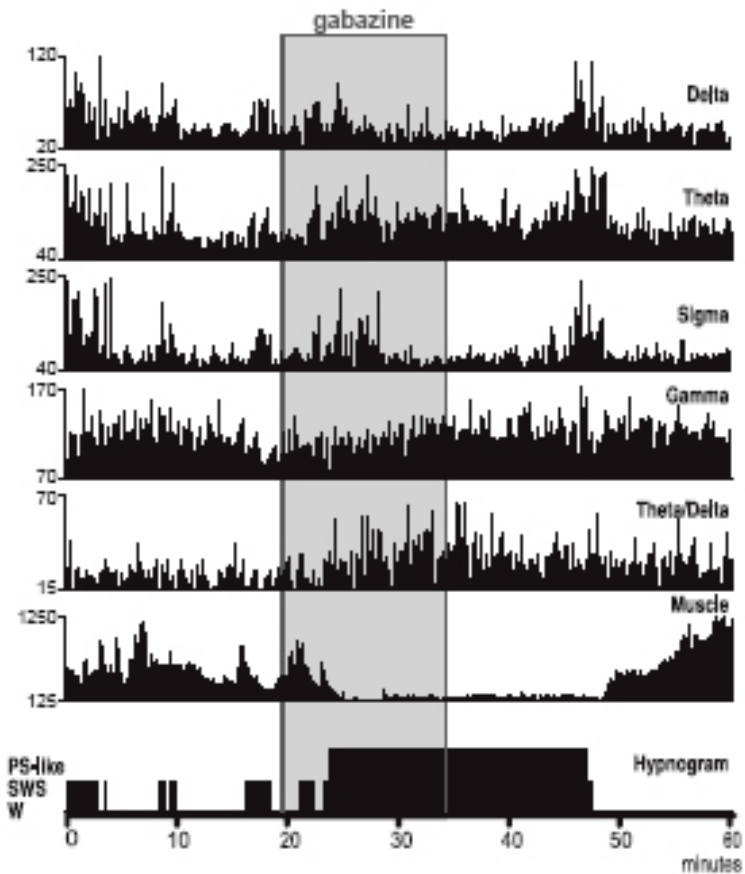
Hypnogram (bottom), EMG and EEG frequency band activities (top) per 5-s epoch before, during and following a 15 min gabazine ejection (100 nA) into the SLD (rat SLD59). Delta (1.6-4.0 Hz), theta (4.4-8.8 Hz), sigma (9.2-14.4 Hz), gamma (31.6-47.6 Hz) frequency band activities from the frontal cortex, theta/delta ratio, and EMG are displayed as amplitude units (μV) or ratios scaled to maximum. Two vertical bars indicate the onset and offset of the gabazine ejection. Note the complete disappearance of the muscular activity and the increased theta and gamma activities during the gabazine effect.
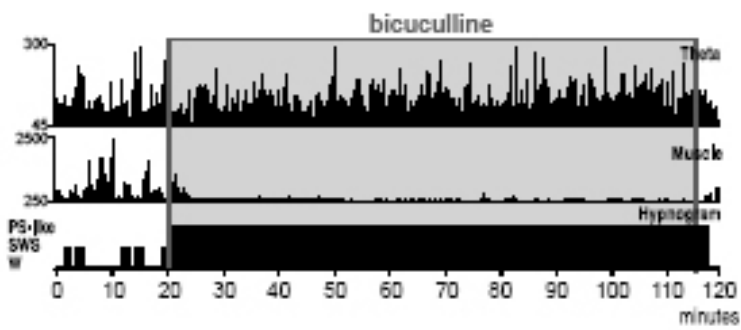
Figure 3:
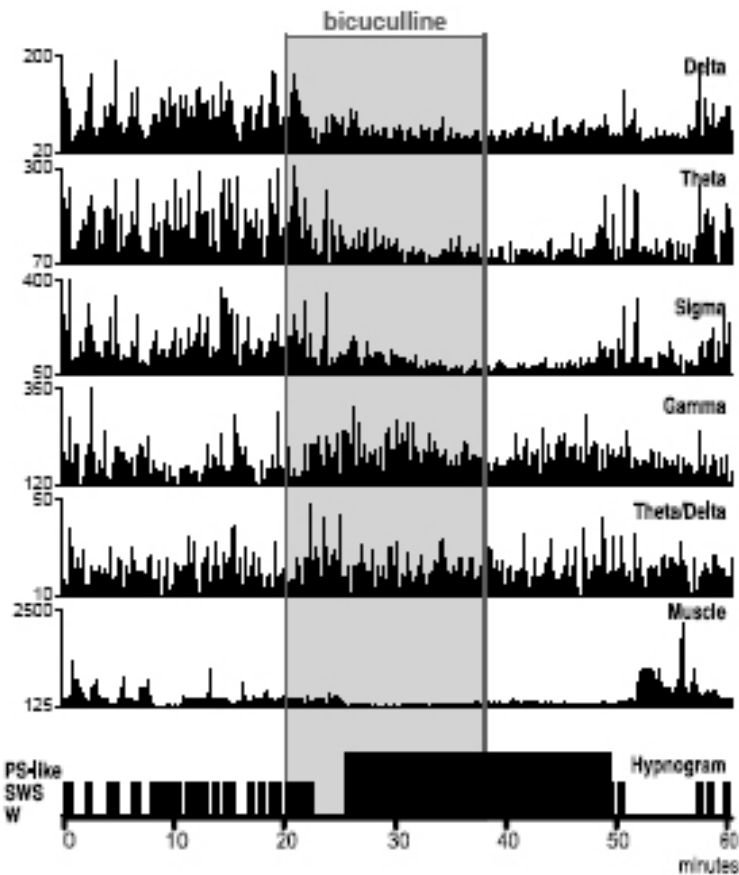
Hypnogram (bottom), EMG and EEG frequency band activities (top) per 5-s epoch before, during and following a bicuculline ejection (100 nA) (rat SLD20) in the SLD. Delta (1.6-4.0 Hz), theta (4.4-8.8 Hz), sigma (9.2-14.4 Hz), gamma (31.6-47.60 Hz) frequency band activities from the frontal cortex, theta/delta ratio, and EMG are displayed as amplitude units (μV) or ratios scaled to maximum. Two vertical bars indicate the onset and offset of the bicuculline ejection. Note the complete disappearance of the muscular activity, the decrease in slow wave activity and the increase in gamma activity during the bicuculline effect.
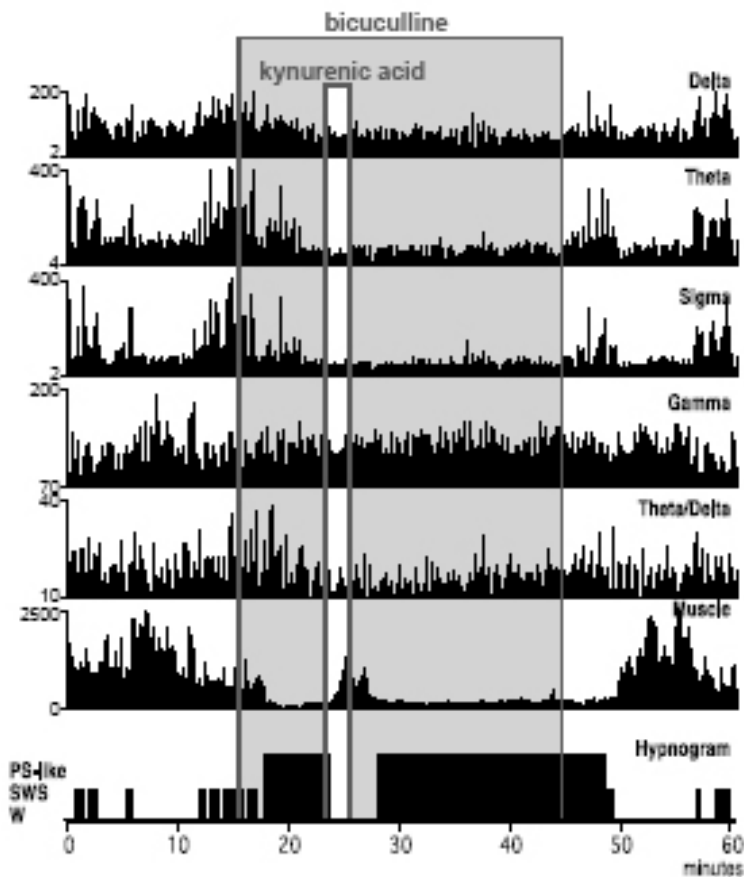
Figure 4:

Hypnogram (bottom), EMG and EEG frequency band activities (top) per 5-s epoch before, during and following a carbachol ejection (200 nA) (rat SLD56) in the SLD. Delta (1.6-4.0 Hz), theta (4.4-8.8 Hz), sigma (9.2-14.4 Hz), gamma (31.6-47.60 Hz) frequency band activities from the frontal cortex, theta/delta ratio, and EMG are displayed as amplitude units (μV) or ratios scaled to maximum. Two vertical bars indicate the onset and offset of the carbachol ejection. Note the increase of the muscle tone with phasic EMG activity and the disappearance of the slow wave activity induced by the carbachol application.
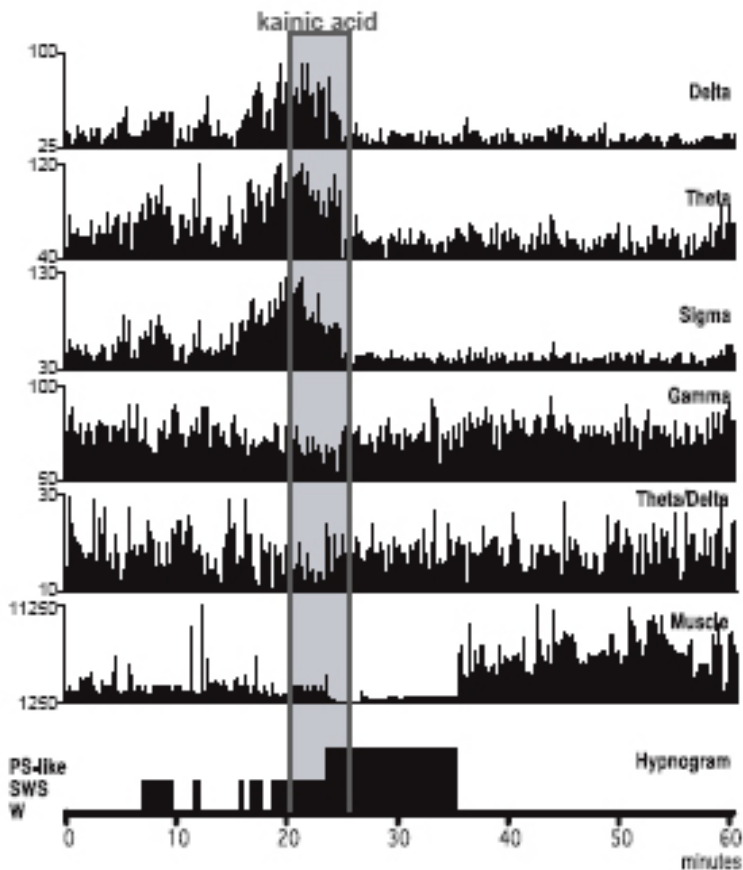
Figure 5:

Hypnogram (bottom), EMG and theta frequency band activities (top) per 5-s epoch before, during and following a 90 min bicuculline ejection (100 nA) into the SLD (rat SLD18). The theta (4.4-8.8 Hz) frequency band activity from the frontal cortex and the EMG are displayed as amplitude units (μV). Two vertical bars indicate the onset and offset of the bicuculline ejection. Note the complete disappearance of muscle activity and the increased theta activity induced by the prolonged bicuculline administration.

Figure 6 :

Hypnogram (bottom), EMG and EEG frequency band activities (top) per 5-s epoch before, during and following bicuculline (100 nA, 37 min 50 s) (rat SLD50) and kynurenic acid (100 nA, 3 min) ejections into the SLD. Delta (1.6-4.0 Hz), theta (4.4-8.8 Hz), sigma (9.2-14.4 Hz), gamma (31.6-47.60 Hz) and theta/delta ratio frequency band activities from the frontal cortex and EMG are displayed as amplitude units (μV) or ratios scaled to maximum. The vertical bars indicate the onset and offset of the ejections. Note the complete muscle atonia and the decrease in the slow wave activity induced by the bicuculline application. When kynurenic acid is applied in addition to bicuculline, the muscle tone rapidly increased back to its pre-bicuculline value while the EEG is not modified.

Figure 7:

Hypnogram (bottom), EMG and EEG frequency band activities (top) per 5-s epoch before, during and following a kainic acid ejection (100 nA, 5 min) (rat SLD09) into the SLD. Delta (1.6-4.0 Hz), theta (4.4-8.8 Hz), sigma (9.2-14.4 Hz), gamma (31.6-47.60 Hz) and theta/delta ratio frequency band activities from the frontal cortex and EMG are displayed as amplitude units (μV) or ratios scaled to maximum. Two vertical bars indicate the onset and offset of the kainic acid ejection. Note the complete disappearance of the muscle tone and slow wave activity induced by the application of kainic acid. Note also the long-lasting rebound of the muscular activity after the muscle atonia.

Figure 8:
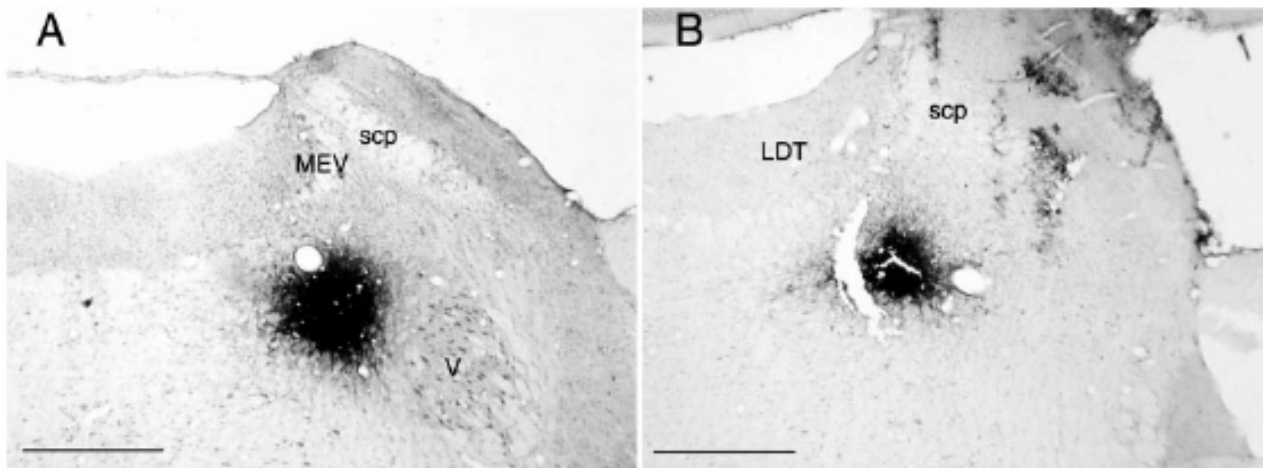
A: Photomicrograph illustrating a PHA-L injection site in the caudal part of the SLD at the level of the rostral trigeminal motor nucleus (V) (rat SLD 21). **B:** Photomicrograph illustrating a CTb injection site in the rostral SLD just rostral to the trigeminal motor nucleus (rat SLD 24). Bars=1mm. Abbreviations: LDT, laterodorsal tegmental nucleus; MEV, mesencephalic trigeminal nucleus; scp, superior cerebellar peduncle; V, motor nucleus of the trigeminal nerve.

Figure 9:
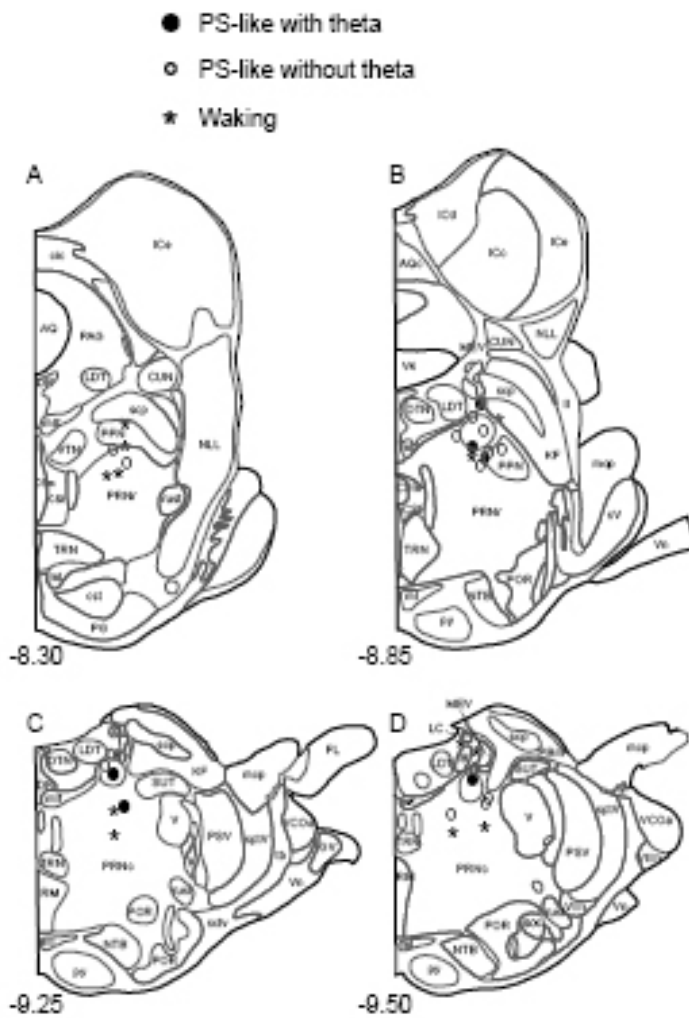
Schematic representation of bicuculline, gabazine, kainic acid and carbachol injection sites. Line drawings of coronal sections at four different levels of the brainstem are from the stereotaxic atlas of Swanson (1992). Each symbol represents one injection site labelled with CTb, PHAL, PSB or C-Fos. Black circles indicate the sites where bicuculline or gabazine induced a PS-like state with theta, and open circle indicate the sites where bicuculline or gabazine induced a PS-like without theta. Stars indicate the sites where bicuculline or gabazine induced waking. Abbreviations: AQ, cerebral aqueduct; Aqc, cerebral aqueduct, collicular recess; B, Barrington's nucleus; cic, commissure of the inferior colliculus; CSl, lateral superior central nucleus raphé; CSm, medial superior central nucleus raphé; cst, corticospinal tract; CUN, cuneiform nucleus; DR, dorsal nucleus raphé; DTN, dorsal tegmental nucleus; ICd, inferior colliculus, dorsal nucleus; ICe, inferior colliculus, external nucleus; FL, flocculus; GV, trigeminal ganglion; KF, Kölliker-Fuse subnucleus;

LC, locus coeruleus nucleus; LDT, laterodorsal tegmental nucleus; ll, lateral lemniscus; mcp, middle cerebellar peduncle; MEV, mesencephalic nucleus of the trigeminal; ml, medial lemniscus; mlf, medial longitudinal fascicle; NLL, nucleus of the lateral lemniscus; NTB, nucleus of the trapezoid body; PAG, periaqueductal gray; PBm, medial parabrachial nucleus; PG, pontine gray; POR, periolivary nuclei; PPN, pedunculopontine nucleus; PRNc, caudal pontine reticular nucleus; PRNr, rostral pontine reticular nucleus; PSV, principal sensory nucleus of the trigeminal; py, pyramidal tract; RM, nucleus raphé magnus; rust, rubrospinal tract; scp, superior cerebellar peduncle; sctv, ventral spinocerebellar tract; SOCl, lateral superior olivary complex; sptV, spinal tract of the trigeminal nerve; SUT, supratrigeminal nucleus; sV, sensory root of the trigeminal nerve; tb, trapezoid body; TRN, tegmental reticular nucleus; V, motor nucleus of the trigeminal nerve; V4, 4th ventricle; VCOa, anterior ventral cochlear nucleus; VIIn, facial nerve; VIIIn, vestibulocochlear nerve; Vn, trigeminal nerve; VTN, ventral tegmental nucleus.

Figure 10:
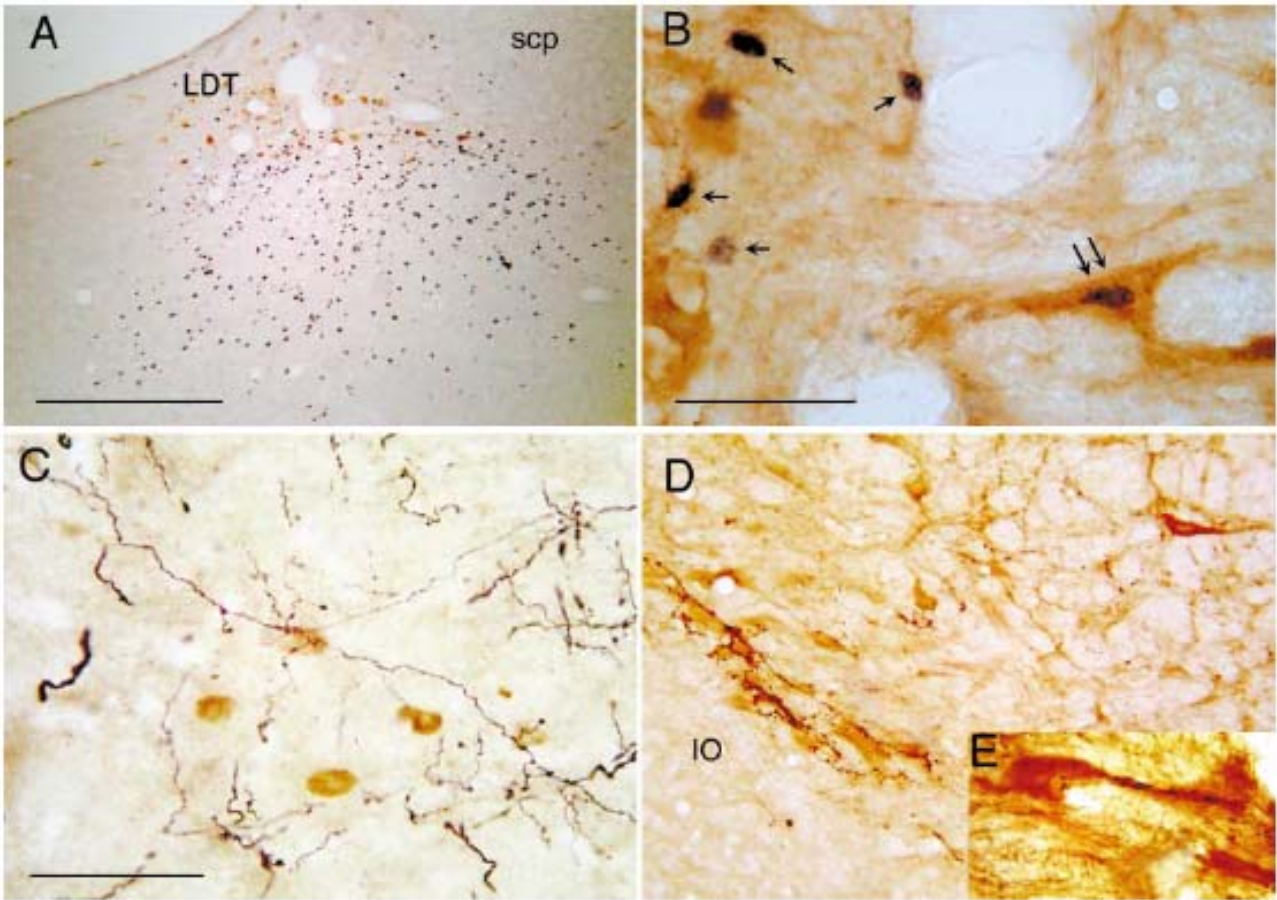
A: Photomicrograph showing a frontal section double-labelled with ChAT (in brown) and C-Fos (in black) immunohistochemistry in an animal that received a 90 min bicuculline injection into the SLD just before perfusion. Numerous C-Fos labelled cells are visible in the SLD just ventral to the LDT, which contains single stained ChAT neurones. Bar = 500µm. **B:** Photomicrograph showing the magnocellular reticular nucleus on a frontal section double-labelled with C-Fos (in black) and glycine (in brown) immunohistochemistry in another animal injected with bicuculline for 90 min bicuculline before perfusion. One double-labelled and several C-Fos singly labelled neurones are visible. Bar = 50µm. **C:** Photomicrograph showing the magnocellular reticular nucleus on a frontal section double-labelled with C-Fos (in brown) and PHA-L (in black) immunohistochemistry in an animal with a PHA-L injection in a bicuculline positive site in the SLD and a 90 min bicuculline injection in the same site 10 days later just before perfusion. Numerous anterogradely labelled varicose fibers cover the MARN, which also contained several C-Fos immunoreactive neurones. Several varicosities from an anterogradely labelled fiber can be seen over a C-Fos labelled nucleus

from a MARN neuron. Bar = 50µm. **D, E:** Photomicrographs showing the MARN on two different frontal sections double-labelled with glycine (in brown) and PHA-L (in black) immunohistochemistry in two different animals with a PHA-L injection in a bicuculline positive site in the SLD. In D, a large contingent of anterogradely labelled varicose fibers is apposed on glycinergic neurones localized in the MARN just dorsal to the inferior olivary complex (SLD 25). In E, varicosities of anterogradely labelled fibers are apposed on the proximal dendrite of a glycine-immunoreactive neuron and one varicosity is apposed on the soma of the neuron (E11). Bars = 100µm in D and 20µm in E. Abbreviations: IO, inferior olive; LDT, laterodorsal tegmental nucleus; scp, superior cerebellar peduncle.

Figure 11:
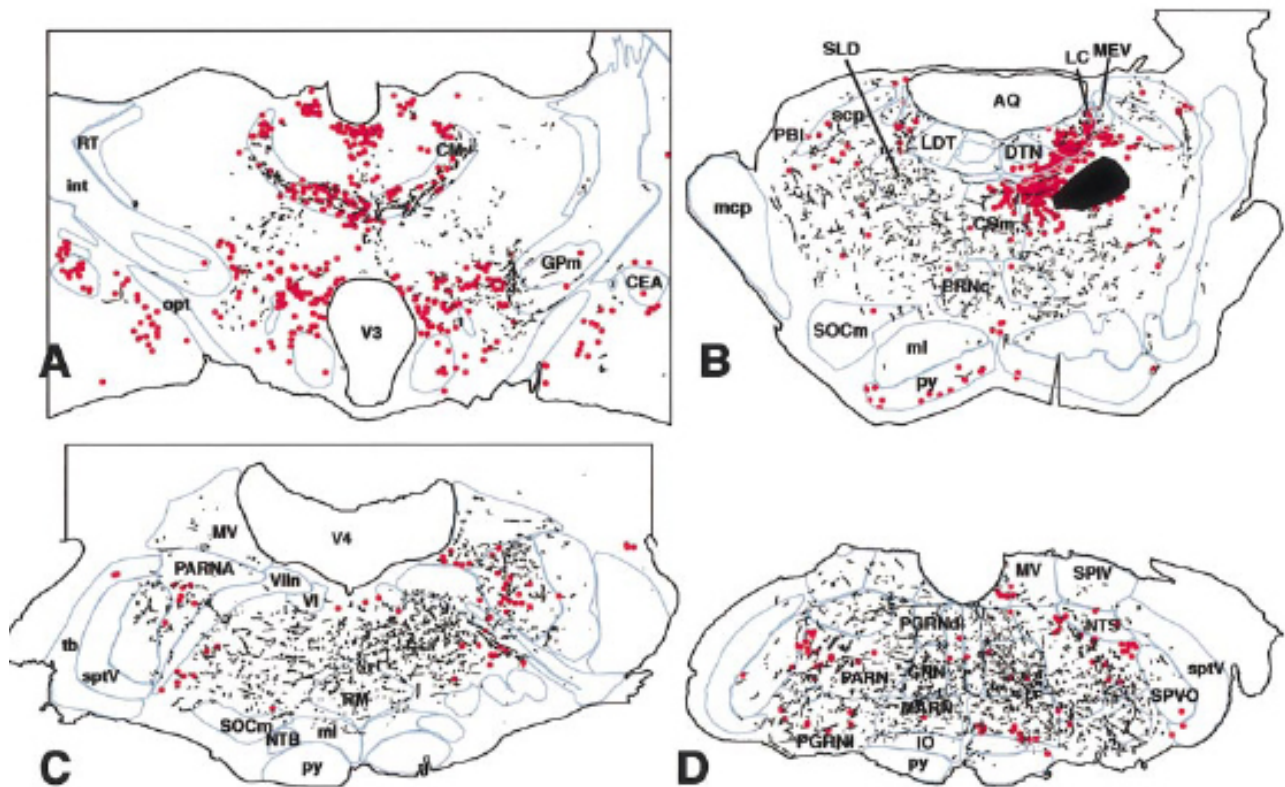
Schematic drawings of PHA-L labelled fibers (in black) and C-Fos labelled neurones (red dots) on frontal sections from hypothalamic to medullary levels from an animal that received a PHA-L injection in a bicuculline positive site in the SLD and a 90 min injection of bicuculline in the same site just before perfusion (rat SLD 50). Abbreviations: AQ, aqueduct of Sylvius; CEA, central nucleus amygdala; CM, central medial nucleus thalamus; CSm, médial superior central nucleus raphé; DTN, dorsal tegmental nucleus; GPm, medial globus pallidus; GRN, gigantocellular reticular nucleus; int, internal capsule; IO, inferior olivary complex; LC, locus coeruleus; LDT, laterodorsal tegmental nucleus; MARN, magnocellular reticular nucleus; mcp, middle cerebellar peduncle; MEV, mesencephalic trigeminal nucleus; ml, medial lemniscus; MV, medial vestibular nucleus; NTB, nucleus of the trapezoid body; NTS, nucleus of the solitary tract; opt, optic tract; PARN, parvicellular reticular nucleus; PARNA, parvicellular reticular nucleus alpha; PBl, lateral parabrachial nucleus; PGRNd, dorsal paragigantocellular reticular nucleus; PGRNl, lateral paragigantocellular reticular nucleus; PRNc, caudal pontine reticular nucleus; py, pyramidal tract;

RM, nucleus raphe magnus; RT, reticular nucleus thalamus; scp, superior cerebellar peduncle; SLD, sublaterodorsal nucleus; SOCm, medial superior olivary complex; SPIV, spinal vestibular nucleus; sptV, spinal tract of the trigeminal nerve; SPVO, spinal trigeminal nucleus, oral part; tb, trapezoid body; V3, 3rd ventricle; V4, 4th ventricle; VI, abducens nucleus; VIIn, facial nerve.

Figure 12:
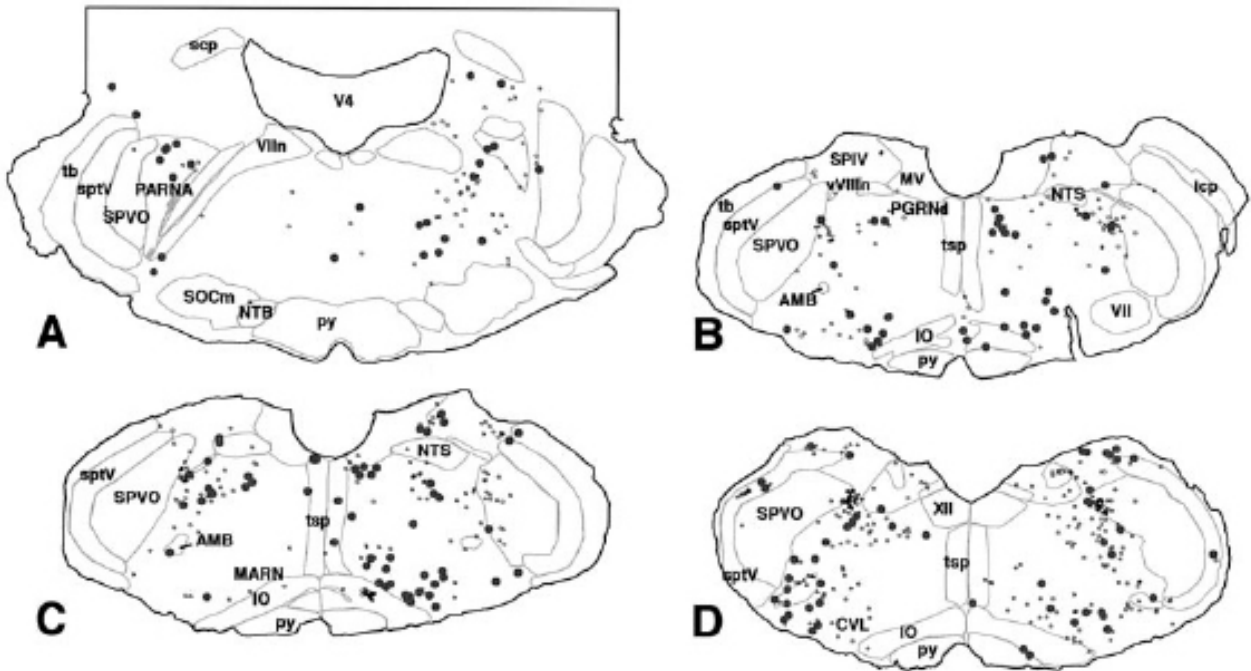
Schematic drawings of C-Fos singly (open circles) and C-Fos/glycine double labelled cells (red dots) on frontal medullary sections from an animal which received just before perfusion a 90 min bicuculline injection into the SLD. Abbreviations: AMB, nucleus ambiguus; CVL, caudoventrolateral reticular nucleus; icp, inferior cerebellar peduncle; IO, inferior olivary complex; MARN, magnocellular reticular nucleus; MV, medial vestibular nucleus; NTB, nucleus of the trapezoid body; NTS, nucleus of the trapezoid body; PARNA, parvicellular reticular nucleus alpha; PGRNd, dorsal paragigantocellular reticular nucleus; py, pyramidal tract; scp, superior cerebellar peduncle; SOCm, medial superior olivary complex; sptV, spinal tract of the trigeminal nerve; SPVO, oral spinal trigeminal nucleus; SPIV, spinal vestibular nucleus; tb, trapezoid body; tsp, tectospinal pathway; V4, 4th ventricle; VII, facial nucleus; VIIn, facial nerve; vVIIIn, vestibular nerve; XII, hypoglossal nucleus.

Table 1. EEG bands amplitudes and EMG amplitude of 5-s epochs during control W, SWS, PS and pharmacological ejections. Values are given as mean±SEM.

	Delta	Theta	Theta/Delta	Sigma	Beta1	Beta2	Gamma	Muscle
Bic/Gbz ejections								
PS-like with θ /n=11								
Bic/Gbz effect	0.16±0.02	0.38±0.02	2.83±0.34	0.16±0.01	0.07±0.01	0.12±0.01	0.08±0.01	1902.63±179.68
PS	0.08±0.01***	0.56±0.02***	9.68±1.52***	0.12±0.01**	0.05±0.00***	0.1±0.01	0.08±0.01	1873.68±191.19
W	0.14±0.01	0.26±0.01***	1.93±0.14*	0.14±0.00	0.09±0.01*	0.18±0.01***	0.16±0.01***	8598.68±973.56***
SWS	0.29±0.02***	0.3±0.01***	1.17±0.12***	0.19±0.01*	0.08±0.01	0.07±0.00***	0.03±0.00***	3789.47±289.87***
PS-like without θ /n=17								
Bic/Gbz effect	0.13±0.02	0.24±0.01	2.23±0.18	0.15±0.01	0.08±0.00	0.19±0.01	0.18±0.02	2044.57±215.93
PS	0.07±0.01***	0.47±0.02***	7.95±0.61***	0.13±0.00**	0.06±0.00***	0.14±0.01**	0.12±0.01**	1946.74±221.75
W	0.12±0.01	0.25±0.01	2.25±0.12	0.14±0.01	0.09±0.01	0.19±0.01	0.17±0.01	8695.65±965.42***
SWS	0.28±0.02***	0.29±0.01***	1.1±0.06***	0.18±0.01**	0.1±0.01	0.07±0.00***	0.04±0.00***	3260.87±276.51**
Carb ejections /n=9								
Carb effect	0.15±0.02	0.36±0.03	2.75±0.37	0.13±0.01	0.06±0.01	0.14±0.02	0.12±0.02	12902.78±3030.38
PS	0.05±0.01***	0.52±0.04**	13.01±2.52**	0.12±0.01	0.05±0.01	0.13±0.02	0.1±0.02	1322.22±150.72**
W	0.13±0.01	0.29±0.02*	2.63±0.44	0.14±0.01	0.07±0.00	0.17±0.01*	0.17±0.02*	10755.56±1958.4
SWS	0.27±0.04*	0.31±0.02	1.41±0.23*	0.19±0.02**	0.09±0.01	0.07±0.01***	0.03±0.00***	3161.11±521.85**
Bic/Kyn ejections /n=6								
Kyn effect	0.24±0.01	0.35±0.02	1.48±0.12	0.11±0.01	0.05±0.00	0.12±0.01	0.1±0.01	7141.67±872.12
Bic effect	0.21±0.02	0.38±0.03	1.95±0.27	0.12±0.01	0.05±0.00	0.12±0.01	0.09±0.01	2041.67±269.03***
PS	0.1±0.01***	0.58±0.03***	6.26±0.91***	0.1±0.01	0.04±0.00	0.08±0.01	0.06±0.01*	2127.78±270.08***
W	0.17±0.01***	0.27±0.02*	1.64±0.11	0.14±0.01**	0.08±0.01**	0.17±0.01**	0.13±0.02	6769.44±775.64
SWS	0.35±0.01***	0.3±0.01	0.86±0.05***	0.16±0.01***	0.05±0.00	0.06±0.01***	0.03±0.01***	3744.44±328.1**
KA ejections /n=5								
KA effect	0.19± 0.03	0.29±0.01	1.61±0.19	0.14±0.02	0.08±0.00	0.15±0.01	0.11±0.02	2425±383.16
PS	0.09±0.01**	0.54±0.02***	6.39±0.67***	0.17±0.01	0.6±0.00*	0.07±0.01***	0.05±0.00**	3155±203.01
W	0.15±0.01	0.25±0.02	1.68±0.08	0.13±0.01	0.1±0.01*	0.2±0.01*	0.14±0.01	7785±1050.61**
SWS	0.28±0.02*	0.31±0.01	1.12±0.08*	0.18±0.01	0.07±0.01	0.08±0.02**	0.05±0.01**	4040±226.47**

Delta, theta, sigma, beta1, beta2, and gamma EEG activities are presented as relative amplitude (% of total amplitude), together with the theta/delta ratio, and EMG absolute amplitude (μV). A one-way analysis of variance (ANOVA) was performed with an EEG or EMG measure as the dependant variable and the state as the independent variable. Fisher's least significant differences test was used for post hoc comparisons. p-levels (* $p<0.05$, ** $p<0.01$, *** $p<0.001$) are indicated besides the values from which a value during an effect was found to differ significantly. Abbreviations: Bic/Gbz: Bicuculline and gabazine, Carb: carbachol, Bic/Kyn: Bicuculline and kynurenic acid co-applications, and KA: kainic acid.

Table 2. Number of C-Fos and C-Fos/gly labelled cells counted per section in the main efferents of the SLD in animals with a 90 min ejection of bicuculline, gabazine or NaCl in the SLD.

Structures	C-Fos + (Bic/Gbz ejections)		C-Fos+ (NaCl ejection)	
	Ipsi	contra	ipsi	contra
ILM	86±19*	59.8±16.1**	3.3±1.5	1.5±1.1
LHA	37.8±9.9	35±7.3	38.7±13.5	36.3±8.9
ZI	21±15.6	16.7±6.2	4.3±3.4	8.3±7.3
PF	31.7±10.7	31.7±8.8	15.3±11	8.3±4.1
MRN	99.3±41.9	56.7±22.3	23.3±15.1	27.7±12.2
DR	15±9		7±3	
ventral PAG	32.3±8.1	29±11	25.7±8.8	20.7±4.8
LDT	79±17.1*	8±4.9	11.3±6.6	5±3.6
PRNr	106.3±33.3	24.3±10.8	19±8.7	22.7±15.6
SLD	186.5±72.5*	6±4.2	1.3±0.3	2±1
PRNc	47.3±12.2*	24.7±11.6	1.7±0.9	1.3±0.9
	*12.7±3**	*6.3±3*	*0.3±0.3*	*0.3±0.3*
RM	19.7±9.9		0	
	15±7.2		*0*	
PARNA	19±7.6	8.7±3	1.3±0.7	0.7±0.3
	2.7±1.5	*3.7±1.5*	*0*	*0.3±0.3*
PARN	24.1±3.5*	33.8±6.4*	2.6±1.2	1.3±1
	*5.1±1.1**	*9±1.7**	*0.8±0.4*	*0.1±0.1*
MARN	23.9±3.1**	14.2±3.5	0.7±0.2	0.9±0.5
	*10.1±2**	*6.4±1.7*	*0.3±0.2*	*0.1±0.1*
GRN	2.8±0.7**	0.3±0.2	0	0.2±0.2
	*1.5±0.5***	*0.3±0.2*	*0*	*0.2±0.2*
PGRNd	5.5±0.8**	4.7±2.2	0.3±0.3	0.2±0.2
	*2.3±0.6**	*1.5±0.8*	*0*	*0.2±0.2*
PGRNl	21±3.2*	23.7±5.6*	4.3±2.8	0.7±0.7
	5.7±3.2	*9.3±1.7***	*0.7±0.3*	*0.3±0.3*

Values presented correspond to the mean number (±SEM) of C-Fos and C-Fos and glycine double-labelled cells counted on one section in three animals per condition, ipsilaterally and contralaterally in the principal efferents of the SLD. Counts of double-labelled cells were made only in the nuclei at caudal pontine and medullary levels. They are displayed in italic below the total number of C-Fos labelled neurones counted in these nuclei. An analysis of variance (ANOVA) was performed with the number of C-Fos or C-Fos/gly labelled cells as the dependant variable and the condition as the independent variable. Post-hoc comparisons were performed using Fisher's least significant differences test. p-levels (* $p < 0.05$, ** $p < 0.01$) refer to comparisons with control conditions (ejection of NaCl) on the same side.